

Multi-agent Performative Prediction with Greedy Deployment and Consensus Seeking Agents

Qiang Li, Chung-Yiu Yau, Hoi-To Wai*

September 9, 2022

Abstract

We consider a scenario where multiple agents are learning a common decision vector from data which can be influenced by the agents' decisions. This leads to the problem of multi-agent performative prediction (Multi-PfD). In this paper, we formulate Multi-PfD as a decentralized optimization problem that minimizes a sum of loss functions, where each loss function is based on a distribution influenced by the local decision vector. We first prove the necessary and sufficient condition for the Multi-PfD problem to admit a unique multi-agent performative stable (Multi-PS) solution. We show that enforcing consensus leads to a laxer condition for existence of Multi-PS solution with respect to the distributions' sensitivities, compared to the single agent case. Then, we study a decentralized extension to the greedy deployment scheme [Mendler-Dünner et al., 2020], called the DSGD-GD scheme. We show that DSGD-GD converges to the Multi-PS solution and analyze its non-asymptotic convergence rate. Numerical results validate our analysis.

1 Introduction

Traditional learning/prediction problems are often formulated with the assumption that data follows a *static* distribution, from which a decision vector is sought by solving a corresponding optimization problem. While this assumption holds for 'stationary' tasks such as image classification, many real world tasks are dynamical, involving data that could be influenced by decisions. In the latter case, the predictions are said to be *performative*. Example scenarios include when users are *strategic* [Hardt et al., 2016, Dong et al., 2018, Kleinberg and Raghavan, 2020] such as in training an E-mail spam classifier, where users (including spammers) can adapt to the classifier's rules to evade detection.

A common way to model *performative prediction* is via incorporating decision-dependent distribution in formulating the learning problem [Quiñonero-Candela et al., 2008]. Since the pioneering work by Perdomo et al. [2020], there is a growing literature in analyzing the performative prediction problem, which studied the convergence of learning algorithms to stable point of performative prediction [Mendler-Dünner et al., 2020, Drusvyatskiy and Xiao, 2020, Brown et al., 2022, Li and Wai, 2022, Wood et al., 2021], algorithms to find stationary solution of performative risk [Izzo et al., 2021, 2022, Miller et al., 2021, Ray et al., 2022], update timescales of agent [Zrnic et al., 2021], etc.

Most of the existing works are focused on the single agent (learner) setting. In this paper, we concentrate on the multi-agent performative prediction (Multi-PfD) problem. Here, the agents are *consensus-seeking* who seek a common decision vector that minimizes the sum of loss functions through communications on a graph/network. Such setup arises naturally where each agent acquires data from different subset/population of users, and they desire to seek a common decision vector for maximal generalization performance. For the example of training an E-mail spam classifier, each agent represents a regional server providing services to a subset of users. These users are in general different and may react to their serving agents differently, leading

*Q. Li, C.-Y. Yau and H.-T. Wai are with the Department of Systems Engineering and Engineering Management, The Chinese University of Hong Kong, Hong Kong SAR of China. Emails: {liqiang, cyau, htwai}@se.cuhk.edu.hk

to heterogeneous and decision dependent data distributions. Notably, our setup differs from the recent works in [Narang et al., 2022, Piliouras and Yu, 2022] which consider a game theoretical setup of Multi-PfD; see Fig. 1 and §2.

For the algorithmic model, we study a decentralized extension of the greedy deployment scheme [Mendler-Düner et al., 2020], particularly we concentrate on the decentralized stochastic gradient (DSGD) [Lian et al., 2017] algorithm with greedy deployment (DSGD-GD). Overall, the DSGD-GD scheme emulates a scenario where agents apply DSGD, a standard decentralized learning algorithm, while being *agnostic* to the performative nature of the prediction problem. In particular, upon each iteration, the non-converged local decisions will be deployed directly. Then, agents optimize their decision using stochastic gradient constructed from data with distribution shifted by local decision.

Tackling Multi-PfD with the DSGD-GD scheme yields a practical scenario of performative prediction in the multi-agent setting. We inquire the open questions: *When will the Multi-PfD problem admit a stable and consensual solution? If so, how fast does it take for DSGD-GD to converge to such solution? Does the limited communication in DSGD-GD impair its convergence rate?* We provide affirmative answers to the above. Our idea hinges on adopting the concept of *performative stable* solution [Perdomo et al., 2020], which is a fixed point solution resulted from the interplay between agent(s) and data that react to the agent(s)’ decisions. In particular, we focus on analyzing the multi-agent performative stable (Multi-PS) solution in our problem.

To our best knowledge, this paper provides the first study and analysis of Multi-PfD with consensus seeking agents via a practical DSGD-GD scheme. We highlight the following key contributions:

- We provide a *necessary and sufficient* condition on the sensitivity of decision dependent data distributions for the existence and uniqueness of the Multi-PS solution. An interesting finding is that the Multi-PS solution exists even if some of the performative prediction problems of individual agents are unstable. The consensus seeking behavior in Multi-PfD tends to *stabilize* the problem.
- We study the DSGD-GD scheme and analyze its convergence towards the Multi-PS solution. We first show that the scheme is convergent under the same sufficient condition for existence of Multi-PS solution. With an appropriate step size rule, in expectation, the squared distance between the Multi-PS solution and the iterates decays as $\mathcal{O}(1/t)$, and the squared consensus distance decays as $\mathcal{O}(1/t^2)$, where t is the iteration number. Our fine-grained analysis also reveals that heterogeneous users, poorly connected graph may slow down the convergence of DSGD-GD, but only so in the transient, and the asymptotic rate has a linear speedup property.
- To validate our analysis, we conduct numerical experiments on synthetic data and real data. Particularly, we consider the Gaussian mean estimation on synthetic data to validate our theory, and the logistics regression problem on the `spambase` dataset.

The paper is organized as follows. §2 introduces the Multi-PfD problem and DSGD-GD scheme. §3 presents the theoretical results on Multi-PfD, DSGD-GD together with a proof outline. Finally, §4 shows numerical experiments to validate our analysis. All proofs can be found in the appendix.

Related Works. As mentioned, the main ingredient of DSGD-GD scheme is the classical DSGD algorithm. The latter was introduced in [Ram et al., 2010, Bianchi and Jakubowicz, 2012, Sayed, 2014] and is recently popularized for decentralized learning. Of relevance to our work are [Lian et al., 2017] which demonstrated a linear speed up against centralized SGD, and [Pu et al., 2021] with a refined analysis, also see [Kong et al., 2021, Bars et al., 2022] on the effects of consensus steps and topology. We also mention recent advances to improve the efficiencies of DSGD in [Tang et al., 2018, Lan et al., 2020, Koloskova et al., 2019]. Our analysis entails fresh challenges as the sought Multi-PS solution cannot be described explicitly as an optimal solution to the Multi-PfD problem.

Another line of relevant works pertains to (multi-agent) reinforcement learning whose formulation also entails a decision-dependent distribution. To this end, policy gradient algorithms are analyzed in [Zhang et al., 2020, Karimi et al., 2019], and they have been recently extended to the multi-agent setting [Zhang et al., 2018, Chen et al., 2021]; also see the survey [Zhang et al., 2021]. Most of the above works showed convergence to a stationary point which may not be unique. This is in contrast to our analysis of DSGD-GD which converges to the unique Multi-PS solution.

2 Problem Setup

Consider a scenario where there are n agents connected on an undirected and connected graph $G = (V, E)$ such that $V = \{1, \dots, n\}$, $E \subseteq V \times V$. Note that we include self-loops such that $(i, i) \in E$ for any $i \in V$. Each agent $i \in V$ draws samples from the i th population of users. The latter is characterized by the distribution $\mathcal{D}_i(\boldsymbol{\theta}_i)$ supported on $Z \subseteq \mathbb{R}^p$, $p \in \mathbb{N}$ and parameterized by the agent's decision vector $\boldsymbol{\theta}_i \in \mathbb{R}^d$, $d \in \mathbb{N}$. In other words, the i th population of users are only influenced by the i th agent's decision vector. Note that the populations of users can be *heterogeneous* such that $\mathcal{D}_i(\boldsymbol{\theta}) \neq \mathcal{D}_j(\boldsymbol{\theta}')$, $i \neq j$, even if $\boldsymbol{\theta} = \boldsymbol{\theta}'$.

The agents aim to find a *common decision vector* $\boldsymbol{\theta} \in \mathbb{R}^d$ in a collaborative fashion that minimizes the average of local losses. Consider the *multi-agent performative prediction (Multi-PfD) problem*:

$$\min_{\boldsymbol{\theta}_i \in \mathbb{R}^d, i=1, \dots, n} \frac{1}{n} \sum_{i=1}^n \mathbb{E}_{Z_i \sim \mathcal{D}_i(\boldsymbol{\theta}_i)} [\ell(\boldsymbol{\theta}_i; Z_i)] \quad \text{s.t.} \quad \boldsymbol{\theta}_i = \boldsymbol{\theta}_j, \forall (i, j) \in E. \quad (1)$$

Since G is connected, the constraint $\boldsymbol{\theta}_i = \boldsymbol{\theta}_j$ for $(i, j) \in E$ enforces the decision to be in *consensus* across the n agents. In the above, $\ell(\boldsymbol{\theta}_i; Z_i)$ is the loss function of the fitness of the decision vector $\boldsymbol{\theta}_i$ with respect to (w.r.t.) the sample Z_i . The expected value $\mathbb{E}_{Z_i \sim \mathcal{D}_i(\boldsymbol{\theta}_i)} [\ell(\boldsymbol{\theta}_i; Z_i)]$ corresponds to the loss at agent i w.r.t. the samples from the i th population of users.

Example 1. We describe a strategic binary classification problem with linear utility for users to illustrate the application of (1). The sample Z_i is defined by a tuple $Z_i = (\mathbf{X}_i, Y_i) \in \mathbb{R}^d \times \{0, 1\}$ of feature and binary label, and the loss function is taken as the logistic regression function:

$$\ell(\boldsymbol{\theta}; Z_i) = \log(1 + \exp(\langle \mathbf{X}_i | \boldsymbol{\theta} \rangle)) - Y \langle \mathbf{X}_i | \boldsymbol{\theta} \rangle + \frac{\beta}{2} \|\boldsymbol{\theta}\|^2, \quad (2)$$

where $\beta > 0$ is a regularization parameter. The above loss function quantifies the mismatches between the classifier $\boldsymbol{\theta}$ and the given data tuple $Z_i = (\mathbf{X}_i, Y_i)$.

On the other hand, the distribution $\mathcal{D}_i(\boldsymbol{\theta}_i)$ is controlled by the i th population of users. The distribution is decision dependent such that the sample $Z_i \sim \mathcal{D}_i(\boldsymbol{\theta}_i)$ depends on the i th decision $\boldsymbol{\theta}_i$. Observing the i th decision $\boldsymbol{\theta}_i$, users of the i th population provides samples that are modified via a linear utility such that $Z_i = (\mathbf{X}_i, Y_i) \sim \mathcal{D}_i(\boldsymbol{\theta}_i)$ is given by

$$\mathbf{X}_i = \arg \max_{\hat{\mathbf{X}} \in \mathbb{R}^d} \left\{ \langle \boldsymbol{\theta}_i | \hat{\mathbf{X}} \rangle - \frac{1}{2\epsilon_i} \|\hat{\mathbf{X}} - \mathbf{X}\|^2 \right\}, \quad Y_i = Y \quad \text{with} \quad (\mathbf{X}, Y) \sim \mathcal{D}_i^\circ, \quad (3)$$

for some $\epsilon_i > 0$, where \mathcal{D}_i° is a base data distribution of the i th population. Note that in the above, we have the closed form solution $\mathbf{X}_i = \mathbf{X} + \epsilon_i \boldsymbol{\theta}_i$. Tackling (1) leads to a common classifier $\bar{\boldsymbol{\theta}}$ which takes the effects of the heterogeneous decision dependent distributions into account.

The Multi-PfD problem (1) comprises of a stochastic objective function with a decision dependent distribution. In particular, for each agent i , the distribution $\mathcal{D}_i(\boldsymbol{\theta}_i)$ captures a feedback mechanism where users of the i th population react to the decision made by the i th agent. See Fig. 1 (left) for an illustration. Due to non-convexity, the performative risk in (1) can be difficult to minimize. In this paper, we are interested in the *multi-agent performative stable* (Multi-PS) solution:

$$\boldsymbol{\theta}^{PS} = \mathcal{M}(\boldsymbol{\theta}^{PS}) := \arg \min_{\boldsymbol{\theta} \in \mathbb{R}^d} \frac{1}{n} \sum_{i=1}^n \mathbb{E}_{Z_i \sim \mathcal{D}_i(\boldsymbol{\theta}^{PS})} [\ell(\boldsymbol{\theta}; Z_i)] \quad (4)$$

which approximately solves (1). Notice that $\boldsymbol{\theta}^{PS}$ is defined to be a fixed point of the map $\mathcal{M} : \mathbb{R}^d \rightarrow \mathbb{R}^d$. The existence and uniqueness of $\boldsymbol{\theta}^{PS}$ will be shown under mild condition in Proposition 1.

Comparison to Existing Works. Our setup differs from recent works in [Piliouras and Yu, 2022, Narang et al., 2022]. Unlike ours, both works considered a game theoretical setting where the agents do not directly communicate their decisions. Instead, agents are coupled through the data distributions which depend on the global decision profile $\vartheta := (\boldsymbol{\theta}_1, \dots, \boldsymbol{\theta}_n)$.

In [Narang et al., 2022], agent/player i seeks to solve $\min_{\boldsymbol{\theta}_i} \mathbb{E}_{Z_i \sim \mathcal{D}_i(\vartheta)} [\ell_i(\boldsymbol{\theta}_i; Z_i)]$ where the local distribution \mathcal{D}_i depends on the global decision ϑ [Fig. 1 (middle)]; while Piliouras and Yu [2022] study a slightly different setting where the goal of agent/player i is to solve $\min_{\boldsymbol{\theta}_i} \mathbb{E}_{Z_i \sim \mathcal{D}(\vartheta)} [\ell(\boldsymbol{\theta}_i; Z_i)]$ [Fig. 1 (right)]. Both works

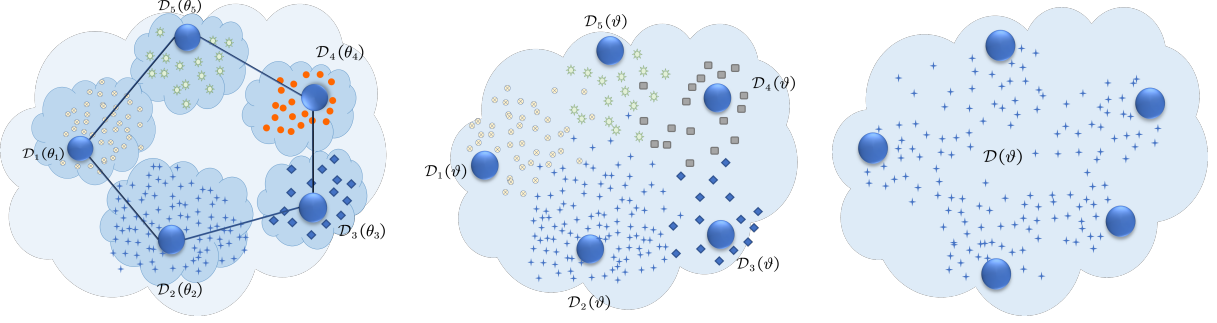


Figure 1: **Comparing the frameworks of multi-agent/player performative prediction.** (Left) [This work](#): agent deploys θ_i and local distribution $\mathcal{D}_i(\theta_i)$ is affected by θ_i only; the agents communicate while aiming to reach consensus $\theta_1 = \dots = \theta_n$ eventually. (Middle) [Narang et al. \[2022\]](#): agent deploys θ_i but local distribution is affected by joint decision $\mathcal{D}_i(\theta_1, \dots, \theta_n)$. (Right) [Piliouras and Yu \[2022\]](#): similar to [Narang et al., 2022] but the distribution is global $\mathcal{D}(\theta_1, \dots, \theta_n)$.

showed convergence to a stable equilibria via (stochastic) gradient-type updates. In contrast, our work considers cooperative agents who are willing to share their decisions with other agents. Under this setting, we show that a natural decentralized scheme achieves convergence to a consensual decision that is performatively stable.

Decentralized Scheme. To find an approximate solution to (1) in a cooperative fashion, the natural approach is to deploy a decentralized scheme where agents communicate limited amount of information with neighbors that are directly connected on G . Furthermore, we focus on a scenario where agents are *agnostic* to that their users may react to the agents' decisions. The above motivates us to study the following variant of the standard DSGD algorithm [[Lian et al., 2017](#)].

Let us define a mixing matrix $\mathbf{W} \in \mathbb{R}_+^{n \times n}$ on G such that $W_{ij} = W_{ji} > 0$ if $(i, j) \in E$, otherwise $W_{ij} = 0$ if $(i, j) \notin E$, satisfying $\sum_{i=1}^n W_{ij} = 1$ for any $i = 1, \dots, n$. We consider the scheme:

DSGD with Greedy Deployment (DSGD-GD) Scheme

At iteration $t = 0, 1, \dots$, for any $i \in V$, agent i updates his/her decision (θ_i^t) by the recursion consisting of two phases

$$\text{(Phase 1)} \quad Z_i^{t+1} \sim \mathcal{D}_i(\theta_i^t) \quad \Bigg| \quad \text{(Phase 2)} \quad \theta_i^{t+1} = \sum_{j=1}^n W_{ij} \theta_j^t - \gamma_{t+1} \nabla \ell(\theta_i^t; Z_i^{t+1}), \quad (5)$$

where $\gamma_{t+1} > 0$ is a step size. Note that $\nabla \ell(\theta_i^t; Z_i^{t+1})$ denotes the gradient taken w.r.t. the first argument θ_i^t , and the samples Z_i^{t+1} at each agent are independent of each other.

The above combines the DSGD algorithm [[Lian et al., 2017](#)] with greedy deployment [[Mendler-Dünnler et al., 2020](#)]. For iteration $t \geq 0$, the scheme can be described with two phases:

In Phase 1, agent i deploys θ_i^t at the i th population, whose users react to the decision and reveal a sample $Z_i^{t+1} \sim \mathcal{D}_i(\theta_i^t)$ to the agent. Note that this is a greedy deployment scheme since the deployed decision θ_i^t may not be stable w.r.t. (1). In Phase 2, agent i receives the current decisions θ_j^t from his/her neighbors $j \in \mathcal{N}_i$ and update θ_i^{t+1} according to the ‘consensus’ + ‘stochastic gradient’ step. Here, the ‘stochastic gradient’ step is based on the local decision θ_i^t and sample Z_i^{t+1} taken in phase one with greedy deployment. We remark that throughout the DSGD-GD scheme, the agents remain unaware of the performative behavior of their users.

Notice that the DSGD-GD scheme can be interpreted as a DSGD algorithm deploying *biased* stochastic gradient updates. Denote $\mathbb{E}_t[\cdot]$ as the conditional expectation up to iteration t , we observe

$$\mathbb{E}_t[\nabla_{\theta_i^t} \ell(\theta_i^t; Z_i^{t+1})] = \mathbb{E}_{Z_i \sim \mathcal{D}_i(\theta_i^t)}[\nabla_{\theta_i^t} \ell(\theta_i^t; Z_i)] \neq \nabla_{\theta_i^t} \{\mathbb{E}_{Z_i \sim \mathcal{D}_i(\theta_i^t)}[\ell(\theta_i^t; Z_i)]\}. \quad (6)$$

The unbiased gradient on the r.h.s. also involves derivative w.r.t. the decision in the distribution. Analyzing the convergence of DSGD-GD therefore requires different techniques.

3 Main Results

This section studies the convergence of the DSGD-GD scheme and demonstrates that the latter can approximately solve the Multi-PfD problem (1). To facilitate our discussions, we first define:

$$f_i(\boldsymbol{\theta}; \bar{\boldsymbol{\theta}}) := \mathbb{E}_{Z_i \sim \mathcal{D}_i(\bar{\boldsymbol{\theta}})}[\ell(\boldsymbol{\theta}; Z_i)], \quad f(\boldsymbol{\theta}; \bar{\boldsymbol{\theta}}) := \frac{1}{n} \sum_{i=1}^n f_i(\boldsymbol{\theta}; \bar{\boldsymbol{\theta}}). \quad (7)$$

Note that the first arguments in f_i, f denote the agent's decision and the second argument is the deployed decision known to the population of users. For the rest of this paper, unless otherwise specified, $\nabla \ell(\boldsymbol{\theta}; Z)$, $\nabla f_i(\boldsymbol{\theta}; \boldsymbol{\theta}')$, $\nabla f(\boldsymbol{\theta}; \boldsymbol{\theta}')$ denote the gradients taken w.r.t. the first argument $\boldsymbol{\theta}$.

Using the above notations, (1) is equivalent to $\min_{\boldsymbol{\theta}} f(\boldsymbol{\theta}; \boldsymbol{\theta})$. We consider the set of assumptions:

A1. Fix any $\bar{\boldsymbol{\theta}} \in \mathbb{R}^d$, the function $f(\boldsymbol{\theta}; \bar{\boldsymbol{\theta}})$ is μ -strongly convex in $\boldsymbol{\theta}$ such that

$$f(\boldsymbol{\theta}'; \bar{\boldsymbol{\theta}}) \geq f(\boldsymbol{\theta}; \bar{\boldsymbol{\theta}}) + \langle \nabla f(\boldsymbol{\theta}; \bar{\boldsymbol{\theta}}) | \boldsymbol{\theta}' - \boldsymbol{\theta} \rangle + (\mu/2) \|\boldsymbol{\theta}' - \boldsymbol{\theta}\|^2, \quad \forall \boldsymbol{\theta}', \boldsymbol{\theta} \in \mathbb{R}^d. \quad (8)$$

A2. For any $i = 1, \dots, n$, the loss function $\ell(\boldsymbol{\theta}; z)$ is L -smooth such that

$$\|\nabla \ell(\boldsymbol{\theta}; z) - \nabla \ell(\boldsymbol{\theta}'; z')\| \leq L\{\|\boldsymbol{\theta} - \boldsymbol{\theta}'\| + \|z - z'\|\}, \quad \forall \boldsymbol{\theta}', \boldsymbol{\theta} \in \mathbb{R}^d, z, z' \in Z. \quad (9)$$

A3. For any $i = 1, \dots, n$, there exists a constant $\epsilon_i > 0$ such that

$$\mathcal{W}_1(\mathcal{D}_i(\boldsymbol{\theta}), \mathcal{D}_i(\boldsymbol{\theta}')) \leq \epsilon_i \|\boldsymbol{\theta} - \boldsymbol{\theta}'\|, \quad \forall \boldsymbol{\theta}', \boldsymbol{\theta} \in \mathbb{R}^d, \quad (10)$$

where $\mathcal{W}_1(\mathcal{D}, \mathcal{D}')$ denotes the Wasserstein-1 distance between the distributions $\mathcal{D}, \mathcal{D}'$.

A1, A2 require the loss functions to be strongly convex and smooth, while A3 states that the amount of distribution shift caused by the reaction of i th population to the agent's decision grows linearly with difference in decision. These assumptions are standard in the literature, e.g., [Perdomo et al., 2020, Mendler-Dünger et al., 2020, Drusvyatskiy and Xiao, 2020]. To simplify notations, we define the average, maximum sensitivity as $\epsilon_{\text{avg}} := \sum_{i=1}^n \epsilon_i/n$, $\epsilon_{\text{max}} := \max_{i=1, \dots, n} \epsilon_i$, respectively.

Our first result establishes the existence of the Multi-PS solution $\boldsymbol{\theta}^{PS}$ satisfying $\nabla f(\boldsymbol{\theta}^{PS}; \boldsymbol{\theta}^{PS}) = \mathbf{0}$:

Proposition 1 (Existence and Uniqueness of $\boldsymbol{\theta}^{PS}$). Under A1-A3. Define the map $\mathcal{M} : \mathbb{R}^d \rightarrow \mathbb{R}^d$

$$\mathcal{M}(\boldsymbol{\theta}) = \arg \min_{\boldsymbol{\theta}' \in \mathbb{R}^d} \frac{1}{n} \sum_{i=1}^n f_i(\boldsymbol{\theta}'; \boldsymbol{\theta}) \quad (11)$$

If $\epsilon_{\text{avg}} < \mu/L$, then the map $\mathcal{M}(\boldsymbol{\theta})$ is a contraction with the unique fixed point $\boldsymbol{\theta}^{PS} = \mathcal{M}(\boldsymbol{\theta}^{PS})$. If $\epsilon_{\text{avg}} \geq \mu/L$, then there exists an instance of (11) where $\lim_{T \rightarrow \infty} \|\mathcal{M}^T(\boldsymbol{\theta})\| = \infty$.

See §A for the proof. Note the inverse condition number μ/L yields a *tight* threshold on the sensitivity of the population for the stability of Multi-PfD. Our result can be viewed as the multi-agent extension to [Perdomo et al., 2020, Prop. 4.1]. Notice that while $\boldsymbol{\theta}^{PS}$ may not solve (1), it yields an approximate solution to the latter, depending on the magnitude of ϵ_{avg} ; see [Perdomo et al., 2020].

Our result shows that Multi-PfD has a relaxed requirement for the existence of Multi-PS solution as it only depends on the *average sensitivity* ϵ_{avg} . Consider when ϵ_i exceeds μ/L for the population served by i th agent, now there may not exist a performative stable solution for the *individual* agent [Perdomo et al., 2020]. Meanwhile, by Proposition 1, the *Multi-PS* solution still exists as long as $\epsilon_{\text{avg}} < \mu/L$, e.g., when there are agents in the network with less sensitive users.

We also compare Proposition 1 to [Narang et al., 2022]. Note that the latter considers decision-dependent distributions $\mathcal{D}_i(\boldsymbol{\vartheta})$ with $\boldsymbol{\vartheta} := (\boldsymbol{\theta}_1, \dots, \boldsymbol{\theta}_n)$ involving all decisions, which is different from our setting. Nevertheless, under similar conditions to A1-A3, Narang et al. [2022, Theorem 1] shows the performative stable

equilibria exists if $\sum_{i=1}^n \epsilon_i^2 < \mu^2/L^2$. When $\epsilon_i = \epsilon_{\text{avg}}$, it yields $\epsilon_{\text{avg}} < \mu/(\sqrt{n}L)$ which is more restrictive than the requirement in Proposition 1.

The relaxed condition in Proposition 1 can be attributed to the consensus seeking nature of (1), where agents with less sensitive users serve as mediators that prevent divergence of the map (11).

Convergence Analysis of DSGD-GD Scheme. Next, we focus on analyzing the convergence of the DSGD-GD scheme. We require the following assumptions:

A4. *The non-negative matrix \mathbf{W} is doubly stochastic, i.e., $\mathbf{W}\mathbf{1} = \mathbf{W}^\top\mathbf{1} = \mathbf{1}$. There exists a constant $\rho \in (0, 1]$ such that $\|\mathbf{W} - (1/n)\mathbf{1}\mathbf{1}^\top\|_2 \leq 1 - \rho$.*

A5. *For any $i = 1, \dots, n$ and fixed $\boldsymbol{\theta} \in \mathbb{R}^d$, there exists $\sigma \geq 0$ such that*

$$\mathbb{E}_{Z_i \sim \mathcal{D}_i(\boldsymbol{\theta})} [\|\nabla \ell(\boldsymbol{\theta}; Z_i) - \nabla f_i(\boldsymbol{\theta}; \boldsymbol{\theta})\|^2] \leq \sigma^2(1 + \|\boldsymbol{\theta} - \boldsymbol{\theta}^{PS}\|^2). \quad (12)$$

A4 is a standard assumption on the mixing matrix, for example if G is a connected graph, then \mathbf{W} satisfying the condition can be constructed [Boyd et al., 2004]. Meanwhile, A5 bounds the variance of the ‘stochastic gradient’ $\nabla \ell(\boldsymbol{\theta}; Z_i)$ as the expected value to the latter yields $\mathbb{E}_{Z_i \sim \mathcal{D}_i(\boldsymbol{\theta})} [\nabla \ell(\boldsymbol{\theta}; Z_i)] = \nabla f(\boldsymbol{\theta}; \boldsymbol{\theta})$, where the gradients are taken w.r.t. the first argument $\boldsymbol{\theta}$. Moreover, we assume that:

A6. *For any $i = 1, \dots, n$, there exists $\varsigma \geq 0$ such that*

$$\|\nabla f(\boldsymbol{\theta}; \boldsymbol{\theta}) - \nabla f_i(\boldsymbol{\theta}; \boldsymbol{\theta})\|^2 \leq \varsigma^2(1 + \|\boldsymbol{\theta} - \boldsymbol{\theta}^{PS}\|^2), \quad \forall \boldsymbol{\theta} \in \mathbb{R}^d. \quad (13)$$

It bounds the *heterogeneity* of the locally observed samples. As $\nabla f_i(\boldsymbol{\theta}; \boldsymbol{\theta}) = \mathbb{E}_{Z_i \sim \mathcal{D}_i(\boldsymbol{\theta})} [\nabla \ell(\boldsymbol{\theta}; Z_i)]$, if $\mathcal{D}_i(\boldsymbol{\theta}) = \mathcal{D}_j(\boldsymbol{\theta})$, the constant will be $\varsigma = 0$ when the population associated with each agent produces identically distributed samples with the same deployed decision vector. Otherwise, $\varsigma > 0$ measures degree of heterogeneity across populations. We remark that even when $\mathcal{D}_i(\boldsymbol{\theta}) = \mathcal{D}_j(\boldsymbol{\theta})$, the samples Z_i^{t+1}, Z_j^{t+1} may still not be identically distributed *during the DSGD-GD iterations* since the decision vectors $\boldsymbol{\theta}_i^t, \boldsymbol{\theta}_j^t$ may not be in consensus when $t < \infty$.

A6 also implies $\max_{i=1, \dots, n} \|\nabla f_i(\boldsymbol{\theta}^{PS}; \boldsymbol{\theta}^{PS})\|^2 \leq \varsigma^2$. In fact, as we show in (52) of the appendix, it suffices to prove the convergence of DSGD-GD without A6 as in [Pu et al., 2021, Yuan and Alghunaim, 2021]. We proceed our analysis with A6 to extract a tighter bound especially when ς is small.

In both A5, A6, we allowed the upper bounds to grow with $\mathcal{O}(1 + \|\boldsymbol{\theta} - \boldsymbol{\theta}^{PS}\|^2)$, e.g. A5 is similar to [Pu et al., 2021, Assumption 1]. This is a weaker condition than the commonly assumed uniform bound of $\mathcal{O}(1)$, e.g., in [Lian et al., 2017]. For example, it covers situations when the quadratic components in $\ell(\cdot)$ depends on both Z and $\boldsymbol{\theta}$. Note that this relaxation implies that the variance/heterogeneity can be unbounded, leading to additional challenges in our analysis.

Define the following quantities and constants: fix any $\delta > 0$,

$$\begin{aligned} \bar{\boldsymbol{\theta}}^t &:= (1/n) \sum_{i=1}^n \boldsymbol{\theta}_i^t, \quad \tilde{\boldsymbol{\theta}}^t := \bar{\boldsymbol{\theta}}^t - \boldsymbol{\theta}^{PS}, \quad \boldsymbol{\Theta}_o^t := (\boldsymbol{\theta}_1^t \cdots \boldsymbol{\theta}_n^t) - \bar{\boldsymbol{\theta}}^t \mathbf{1}^\top, \quad \tilde{\mu} := \mu - (1 + \delta)\epsilon_{\text{avg}}L, \\ c_1 &:= \frac{L(1 + \epsilon_{\text{max}})^2}{2n\delta\epsilon_{\text{avg}}}, \quad c_2 := 4 \left(\frac{\sigma^2}{n} + L^2(1 + \epsilon_{\text{max}})^2 \right), \quad c_3 := 12\sigma^2 + 18L^2(1 + \epsilon_{\text{max}})^2. \end{aligned} \quad (14)$$

Note that $\tilde{\boldsymbol{\theta}}^t$ is the distance between the t th averaged iterate $\bar{\boldsymbol{\theta}}^t$ and $\boldsymbol{\theta}^{PS}$, while $\boldsymbol{\Theta}_o^t$ is a $d \times n$ matrix of the t th *consensus error*. The following theorem establishes the convergence rate of DSGD-GD:

Theorem 1. Under A1–A6 and the condition on average sensitivity that $\epsilon_{\text{avg}} < \frac{\mu}{(1+\delta)L}$. Suppose the step sizes $\{\gamma_t\}_{t \geq 1}$ satisfy $\gamma_{t+1} \leq \gamma_t$ for any $t \geq 1$,

$$\sup_{t \geq 1} \gamma_t \leq \min \left\{ \frac{4}{\tilde{\mu}}, \frac{\tilde{\mu}}{c_2}, \frac{\rho}{\sqrt{2c_3}}, \sqrt{\frac{\rho^2 \tilde{\mu}}{192c_1(\sigma^2 + \varsigma^2)}}, \frac{\rho c_1}{4\tilde{\mu}c_1 + \rho c_2} \right\}, \quad (15)$$

and the condition $\frac{\gamma_t}{\gamma_{t+1}} \leq \min\{\sqrt{1 + (\tilde{\mu}/4)\gamma_{t+1}^2}, \sqrt[3]{1 + (\tilde{\mu}/4)\gamma_{t+1}^3}, 1 + \rho/(4 - 2\rho)\}$ for any $t \geq 1$. Then, the iterates generated by DSGD–GD admit the following bound for any $t \geq 0$,

$$\mathbb{E} \left[\|\tilde{\boldsymbol{\theta}}^{t+1}\|^2 \right] \leq \prod_{i=1}^{t+1} \left(1 - \frac{\tilde{\mu}\gamma_i}{2} \right) \mathsf{D} + \frac{288c_1(\sigma^2 + \varsigma^2)}{\rho^2 \tilde{\mu}} \gamma_{t+1}^2 + \frac{8\sigma^2}{\tilde{\mu}n} \gamma_{t+1}, \quad (16)$$

$$\mathbb{E} \left[\frac{1}{n} \|\boldsymbol{\Theta}_o^{t+1}\|_F^2 \right] \leq \left(1 - \frac{\rho}{2} \right)^{t+1} \frac{1}{n} \|\boldsymbol{\Theta}_o^0\|_F^2 + \frac{2(9 + 12\bar{\Delta})(\sigma^2 + \varsigma^2)}{\rho^2} \gamma_{t+1}^2, \quad (17)$$

where $\mathsf{D} := \|\tilde{\boldsymbol{\theta}}^0\|^2 + \gamma_1 \frac{8c_1}{n\rho} \|\boldsymbol{\Theta}_o^0\|_F^2$ denotes the initial error, $\bar{\Delta} := \mathsf{D} + \frac{3}{2} + \frac{8\sigma^2}{c_2 n}$, and we recall the definitions of the constants c_1, c_2, c_3 from (14).

The free parameter $\delta > 0$ in (14) can be chosen arbitrarily. Thus, according to Theorem 1, DSGD–GD converges when the average sensitivity ϵ_{avg} is strictly below the threshold μ/L in Proposition 1, i.e., the same sufficient and necessary condition that guarantees the existence of $\boldsymbol{\theta}^{PS}$. Further, our result holds for general step size rules such as constant step size and diminishing step size.

To yield $\mathbb{E}[\|\tilde{\boldsymbol{\theta}}^t\|^2] \rightarrow 0$, a common option is $\gamma_t = \frac{a_0}{a_1+t}$ for some $a_0, a_1 > 0$. In the latter case as $\gamma_t = \mathcal{O}(1/t)$, we observe from (16), (17) that the distance to performative stable solution $\|\tilde{\boldsymbol{\theta}}^t\|^2$ converges to zero as $\mathcal{O}(1/t)$, while the consensus error $\|\boldsymbol{\Theta}_o^t\|_F^2$ converges to zero as $\mathcal{O}(1/t^2)$. We remark that our analysis also applies to the case of time varying graph; see §G for a proof sketch.

On the other hand, the bound (16) can be simplified to

$$\mathbb{E}[\|\tilde{\boldsymbol{\theta}}^t - \boldsymbol{\theta}^{PS}\|^2] \lesssim \prod_{i=1}^t \left(1 - \frac{\tilde{\mu}\gamma_i}{2} \right) + \frac{L(\sigma^2 + \varsigma^2)}{n\delta\tilde{\mu}\rho^2\epsilon_{\text{avg}}} \gamma_t^2 + \frac{\sigma^2}{n\tilde{\mu}} \gamma_t. \quad (18)$$

As seen, the error is controlled by three terms. The first term is a transient term that consists of the product $\prod_{i=1}^t (1 - \tilde{\mu}\gamma_i)$. It decays sub-geometrically and is scaled by the initial error D . The second term is a transient term and is affected by the spectral gap of mixing matrix ρ , the degree of heterogeneity ς , etc. It decays as $\mathcal{O}(\gamma_t^2)$. Finally, the last term is a fluctuation term that only depends on the averaged noise variance $\mathcal{O}(\sigma^2/n)$. It decays at the slowest rate as $\mathcal{O}(\gamma_t)$.

Effects of Network Topology and Heterogeneity. An interesting observation from (18) is on how the network topology (ρ) and heterogeneity across local sample distribution (ς) affects the convergence behavior of DSGD–GD. First, we note that the last term of $\mathcal{O}(\gamma_t \sigma^2 / (\tilde{\mu}n))$ is similar to the fluctuation term in SGD using the batch size of n under a centralized setting, e.g., [Moulines and Bach, 2011]. Second, the constants ρ, ς only affect the term of rate $\mathcal{O}(\gamma_t^2)$.

In the case with diminishing step size $\gamma_t = \frac{a_0}{a_1+t}$, the second term of (18) will vanish at a faster rate than the last term. Particularly, if for some $C > 0$,

$$\gamma_t \leq C \cdot \delta \rho^2 \epsilon_{\text{avg}} \sigma^2 [L(\sigma^2 + \varsigma^2)]^{-1} \quad (19)$$

then (18) will be dominated by $\mathcal{O}(\gamma_t \sigma^2 / (\tilde{\mu}n))$. In other words, the effects of the network topology and heterogeneous population vanish asymptotically as $\tilde{\boldsymbol{\theta}}^t \rightarrow \boldsymbol{\theta}^{PS}$.

As such, the ‘linear speedup’ behavior of DSGD in [Lian et al., 2017, Pu et al., 2021] can be extended to Multi-PfD with the DSGD–GD scheme. Again, we highlight that the consensus seeking behavior of agents has led to such speedup in convergence towards the Multi-PS solution.

3.1 Proof of Theorem 1

We outline the main steps in proving Theorem 1. As a preparatory step, we borrow the following lemma on the Lipschitzness of $\nabla f_i(\boldsymbol{\theta}, \boldsymbol{\theta})$ from [Drusvyatskiy and Xiao, 2020, Lemma 2.1]:

Lemma 2 (Continuity of ∇f_i). *Under A2, A3. For any $\boldsymbol{\theta}_0, \boldsymbol{\theta}_1, \boldsymbol{\theta}, \boldsymbol{\theta}' \in \mathbb{R}^d$, it holds:*

$$\|\nabla f_i(\boldsymbol{\theta}_0; \boldsymbol{\theta}) - \nabla f_i(\boldsymbol{\theta}_1; \boldsymbol{\theta}')\| \leq L \|\boldsymbol{\theta}_0 - \boldsymbol{\theta}_1\| + L\epsilon_i \|\boldsymbol{\theta} - \boldsymbol{\theta}'\|. \quad (20)$$

By A4, the update recursion for the average iterate of DSGD-GD can be expressed as

$$\bar{\boldsymbol{\theta}}^{t+1} = (1/n) \sum_{i=1}^n \boldsymbol{\theta}_i^{t+1} = \bar{\boldsymbol{\theta}}^t - \gamma_{t+1} \sum_{i=1}^n \nabla \ell(\boldsymbol{\theta}_i^t; Z_i^{t+1})/n. \quad (21)$$

Using the above recursion, we show the following lemma for the one-step progress of DSGD-GD:

Lemma 3. (Descent Lemma) *Fix any $\delta > 0$ and let $\epsilon_{\text{avg}} \leq \frac{\mu}{(1+\delta)L}$. Under A1, A2, A3, A5 and let the step sizes satisfy $\sup_{t \geq 0} \gamma_{t+1} \leq \frac{\tilde{\mu}}{c_2}$, the following bound holds*

$$\mathbb{E}_t \left\| \tilde{\boldsymbol{\theta}}^{t+1} \right\|^2 \leq (1 - \tilde{\mu}\gamma_{t+1}) \left\| \tilde{\boldsymbol{\theta}}^t \right\|^2 + [c_1\gamma_{t+1} + c_2\gamma_{t+1}^2] \frac{1}{n} \left\| \boldsymbol{\Theta}_o^t \right\|_F^2 + \frac{2\sigma^2}{n} \gamma_{t+1}^2, \quad (22)$$

for any $t \geq 0$, where $\mathbb{E}_t[\cdot]$ is the expectation operator conditioned on the iterates up to the t th iteration, and we recall the definitions of $c_1, c_2, \tilde{\mu}$ from (14).

The proof is in §B. We highlight that proving the upper bound (22) requires the smoothness property Lemma 2 for handling the difference $\sum_{i=1}^n \nabla f_i(\boldsymbol{\theta}_i^t, \boldsymbol{\theta}_i^t) - \nabla f_i(\boldsymbol{\theta}^{PS}, \boldsymbol{\theta}^{PS})$ as proportional to the error against the Multi-PS solution $\tilde{\boldsymbol{\theta}}^t$ and the consensus error $\|\boldsymbol{\Theta}_o^t\|_F^2$. Lemma 3 prompts us to study the consensus error $\|\boldsymbol{\Theta}_o^t\|_F^2$ and a key observation is:

Lemma 4. (Consensus Error Bound) *Under A2–A6 and let the step sizes satisfy $\sup_{t \geq 0} \gamma_{t+1} \leq \rho/\sqrt{2c_3}$, then it holds*

$$\mathbb{E}_t \left[\frac{1}{n} \left\| \boldsymbol{\Theta}_o^{t+1} \right\|_F^2 \right] \leq \left(1 - \frac{\rho}{2} \right) \frac{1}{n} \left\| \boldsymbol{\Theta}_o^t \right\|_F^2 + 12[\sigma^2 + \varsigma^2] \frac{\gamma_{t+1}^2}{\rho} \left\| \tilde{\boldsymbol{\theta}}^t \right\|^2 + 9(\sigma^2 + \varsigma^2) \frac{\gamma_{t+1}^2}{\rho}, \quad (23)$$

for any $t \geq 0$, where we recall that $c_3 := 12\sigma^2 + 18L^2(1 + \epsilon_{\max})^2$.

The proof is in §C. In (52) of the appendix, we provide an alternative consensus error bound without using A6. Note that despite the decision dependent distributions due to the performative nature of Multi-PfD, the above bound shows a similar trend as in [Bars et al., 2022, Pu et al., 2021, Kong et al., 2021, Koloskova et al., 2019].

However, unlike [Bars et al., 2022, Lemma 2], the r.h.s. of (23) contains a $\mathcal{O}([\sigma^2 + \varsigma^2]\gamma_{t+1}^2\|\tilde{\boldsymbol{\theta}}^t\|^2)$ term which arises from A5, A6 with the growth condition. This introduces new challenges to analysis as it will be insufficient to conclude from (23) alone that DSGD-GD converges to a consensual solution.

Our plan is to consider Lemmas 3 and 4 simultaneously in order to control $\mathbb{E}\|\tilde{\boldsymbol{\theta}}^t\|^2, \mathbb{E}\|\boldsymbol{\Theta}_o^t\|_F^2$. Define the following sequence of non-negative numbers: for any $t \geq 0$,

$$\mathcal{L}_{t+1} := \mathbb{E} \left[\left\| \tilde{\boldsymbol{\theta}}^{t+1} \right\|^2 + \gamma_{t+1} \frac{8c_1}{\rho n} \left\| \boldsymbol{\Theta}_o^{t+1} \right\|_F^2 \right]. \quad (24)$$

We obtain the following lemma:

Lemma 5 (Convergence of \mathcal{L}_t). *Under A1–A6. Suppose that the step sizes satisfy $\sup_{t \geq 0} \gamma_{t+1} \leq \min \left\{ \frac{4}{\tilde{\mu}}, \sqrt{\frac{\rho^2 \tilde{\mu}}{192c_1(\sigma^2 + \varsigma^2)}}, \frac{\rho c_1}{4\tilde{\mu}c_1 + \rho c_2} \right\}$. For any $t \geq 0$, it holds*

$$\mathcal{L}_{t+1} \leq (1 - \tilde{\mu}\gamma_{t+1}/2) \mathcal{L}_t + \rho^{-2} 72c_1(\sigma^2 + \varsigma^2)\gamma_{t+1}^3 + n^{-1} 2\sigma^2 \gamma_{t+1}^2. \quad (25)$$

Further, if the step sizes satisfy $\frac{\gamma_{t-1}}{\gamma_t} \leq \min\{\sqrt{1 + (\tilde{\mu}/4)\gamma_t^2}, \sqrt[3]{1 + (\tilde{\mu}/4)\gamma_t^3}\}$ for any $t \geq 1$, then

$$\mathbb{E} \left[\left\| \tilde{\boldsymbol{\theta}}^{t+1} \right\|^2 + \gamma_{t+1} \frac{8c_1}{\rho n} \left\| \boldsymbol{\Theta}_o^{t+1} \right\|_F^2 \right] \leq \prod_{i=1}^{t+1} \left(1 - \frac{\tilde{\mu}\gamma_i}{2} \right) D + \frac{288c_1(\sigma^2 + \varsigma^2)}{\rho^2 \tilde{\mu}} \gamma_{t+1}^2 + \frac{8\sigma^2}{\tilde{\mu}n} \gamma_{t+1}, \quad (26)$$

where we recall that $D := \left\| \tilde{\boldsymbol{\theta}}^0 \right\|^2 + \gamma_1 \frac{8c_1}{\rho n} \left\| \boldsymbol{\Theta}_o^0 \right\|_F^2$.

The proof is in §D, where (25) is based on a careful combination of Lemmas 3 and 4, and (26) is computed from the non-asymptotic analysis for the recursion (25).

Proof of Theorem 1. Lemma 5 immediately leads to (16) of the theorem as the l.h.s. of (26) is lower bounded by $\mathbb{E} \left\| \tilde{\boldsymbol{\theta}}^{t+1} \right\|^2$. To obtain (17), we observe from the simplifying the r.h.s. of (26) that

$$\sup_{t \geq 1} \mathbb{E} \left\| \tilde{\boldsymbol{\theta}}^t \right\|^2 \leq D + \frac{288c_1(\sigma^2 + \varsigma^2)}{\rho^2 \tilde{\mu}} \gamma_1^2 + \frac{8\sigma^2}{\tilde{\mu}n} \gamma_1 \leq D + \frac{3}{2} + \frac{8\sigma^2}{c_2 n} =: \bar{\Delta}. \quad (27)$$

Note that $\left\| \tilde{\boldsymbol{\theta}}^0 \right\|^2 \leq \bar{\Delta}$ as well. Substituting the above into Lemma 4 yields

$$\begin{aligned} \frac{1}{n} \mathbb{E} \left\| \boldsymbol{\Theta}_o^{t+1} \right\|_F^2 &\leq (1 - \rho/2) \frac{1}{n} \mathbb{E} \left\| \boldsymbol{\Theta}_o^t \right\|_F^2 + \rho^{-1} (9 + 12\bar{\Delta}) (\sigma^2 + \varsigma^2) \gamma_{t+1}^2 \\ &\leq \left(1 - \frac{\rho}{2} \right)^{t+1} \frac{1}{n} \left\| \boldsymbol{\Theta}_o^0 \right\|_F^2 + \frac{(9 + 12\bar{\Delta})(\sigma^2 + \varsigma^2)}{\rho} \sum_{s=1}^{t+1} \left(1 - \frac{\rho}{2} \right)^{t+1-s} \gamma_s^2 \end{aligned} \quad (28)$$

Applying Lemma 7 in the appendix together with the step size condition $\gamma_t/\gamma_{t+1} \leq 1 + \rho/(4 - 2\rho)$, $t \geq 1$, leads to (17) of the theorem. This concludes our proof. \square

4 Numerical Experiments

We consider two examples of performative prediction problems to verify our theories. All experiments are conducted with Python on a server using 80 threads of an Intel Xeon 6318 CPU.

Multi-agent Gaussian Mean Estimation. We aim to illustrate Proposition 1, Theorem 1 via a scalar Gaussian mean estimation problem on synthetic data. We consider $n = 25$ agents connected on a ring graph, and the Multi-PfD problem (1) is specified with $\ell(\boldsymbol{\theta}_i; Z_i) = (\boldsymbol{\theta}_i - Z_i)^2/2$. The local distributions are given by $\mathcal{D}_i(\boldsymbol{\theta}_i) \equiv \mathcal{N}(\bar{z}_i + \epsilon_i \boldsymbol{\theta}_i, \sigma^2)$, where \bar{z}_i is the mean value to be estimated. For this problem, we have $\mu = 1$, $L = 1$, as such if $0 < \bar{\epsilon} = \epsilon_{\text{avg}} < 1$, the Multi-PS solution can be computed in closed form as $\boldsymbol{\theta}^{PS} = \sum_{i=1}^n \bar{z}_i / [n(1 - \epsilon_{\text{avg}})]$; while $\boldsymbol{\theta}^{PS}$ does not exist if $\epsilon_{\text{avg}} \geq 1$.

In our experiments, we set $\bar{z}_i = 10$, $\sigma^2 = 50$ and step size for DSGD-GD as $\gamma_t = a_0/(a_1 + t)$ with $a_0 = 50$, $a_1 = 10^4$. In Fig. 2, we compare the gap $\left\| \bar{\boldsymbol{\theta}}^t - \boldsymbol{\theta}^{PS} \right\|^2$, consensus error $\left\| \boldsymbol{\Theta}_o^t \right\|^2$, expected performative risk $f(\bar{\boldsymbol{\theta}}^t; \bar{\boldsymbol{\theta}}^t)$ of (1), against the iteration number t . We examine the behavior of DSGD-GD when the Multi-PfD problem has an averaged sensitivity parameter of $\epsilon_{\text{avg}} \in \{0.9, 1.01, 1.05, 1.1\}$ and under a heterogeneous, decision-dependent distribution environment where ϵ_i are distinct.

We first observe from Fig. 2 (left) and (middle) that when $\epsilon_{\text{avg}} = 0.9 < 1$, the gap $\left\| \bar{\boldsymbol{\theta}}^t - \boldsymbol{\theta}^{PS} \right\|^2$ decays at $\mathcal{O}(1/t)$ as $t \rightarrow \infty$, while the consensus error $\left\| \boldsymbol{\Theta}_o^t \right\|^2$ decays at $\mathcal{O}(1/t^2)$. This coincides exactly with Theorem 1. Furthermore, in Fig. 2 (right), we simulate a setting when one of the agents with $\epsilon_i = 1.01$ is always disconnected from the network and perform the greedy deployment scheme *individually*. We observe from the figure that its performative risk $f_i(\boldsymbol{\theta}_i^t; \boldsymbol{\theta}_i^t)$ diverges as $t \rightarrow \infty$. This indicates that consensus can help stabilize the system.

Lastly, from Fig. 2 (middle) and (right), we observe that whenever $\epsilon_{\text{avg}} > 1$, the consensus error and performative risk diverge. Again, this corroborates with our Proposition 1.

Email Spam Classification. We evaluate the performance of DSGD-GD by simulating the performative effects on a real dataset. This example is a multi-agent spam classification task based on `spambase`, a dataset [Hopkins, 1999] with $m = 4601$ samples, $d = 48$ features. We adopt Example 1 and simulate a scenario with

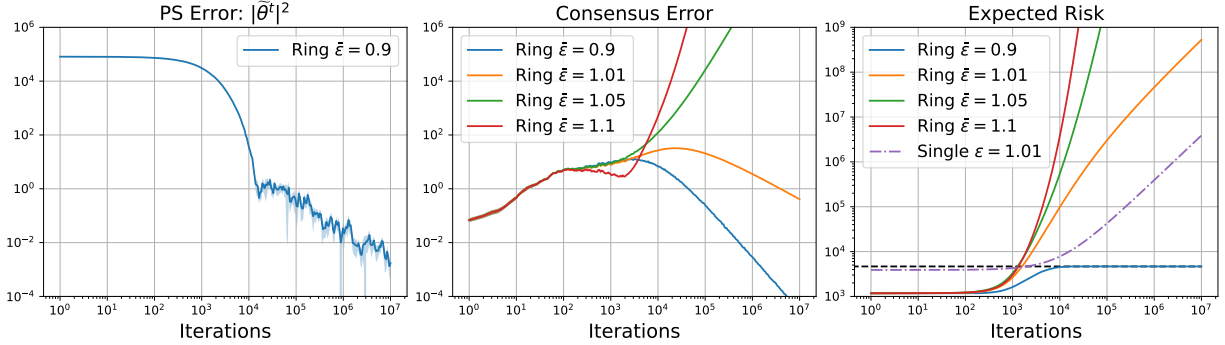


Figure 2: **Multi-agent Gaussian Mean Estimation.** (Left) Gap to Multi-PS solution. Note that θ^{PS} does not exist if $\epsilon_{\text{avg}} \geq 1$ and the plots are thus skipped. (Middle) Consensus error $\|\Theta_o^t\|_F^2$. (Right) Performative risk (7). Results are averaged over 10 runs and shaded area is 90% confidence interval.

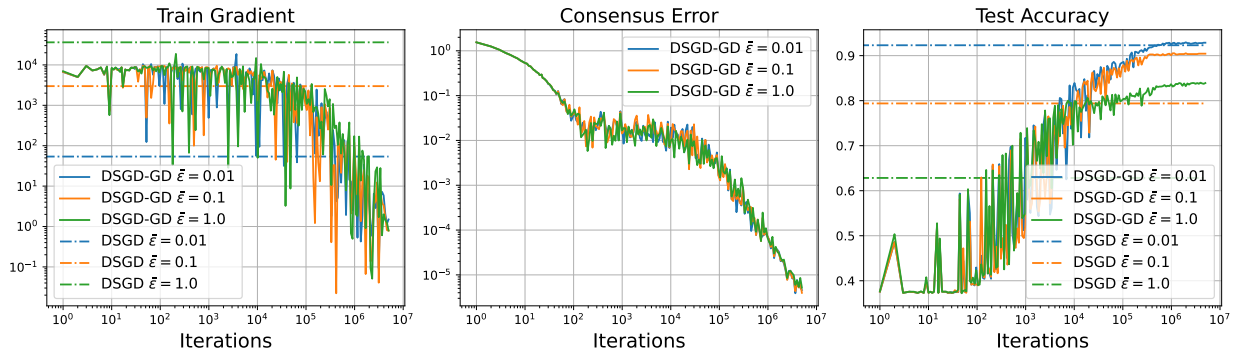


Figure 3: **Spam Email Classification.** (Left) Gradient on training dataset $\|\nabla f(\bar{\theta}^t; \bar{\theta}^t)\|^2$. Note that $\nabla f(\theta^{PS}; \theta^{PS}) = \mathbf{0}$ and thus the gradient norm measures the gap to θ^{PS} . (Middle) Consensus Error. (Right) Test accuracy with shifted distributions. We also compare the non-performative optimal solution (dashed lines, DSGD in the legend) on the shifted dataset.

25 regional servers on a ring graph. Each server has access to training data from $m_i = 138$ samples from `spambase` modeling the different set of users; the rest of $m_{\text{train}} = 1150$ samples are taken as testing data. The servers aim to find a common *spam filter classifier* via (2) with $\beta = 10^{-4}$. To model the strategic behavior of users, their features \mathbf{X}_i are adapted to θ_i through maximizing a linear utility function, resulting in the shifted distribution $\mathcal{D}_i(\theta_i)$ specified in (3). The sensitivity parameters are set as $\epsilon_i \in \{0.4\epsilon_{\text{avg}}, 0.45\epsilon_{\text{avg}}, \dots, 1.6\epsilon_{\text{avg}}\}$ with $\bar{\epsilon} = \epsilon_{\text{avg}} \in \{0.01, 0.1, 1\}$.

Our results are shown in Fig. 3 as we compare the gradient $\|\nabla f(\bar{\theta}^t; \bar{\theta}^t)\|^2$ evaluated on the training dataset, the consensus error $\|\Theta_o^t\|_F^2$, and the accuracy on the testing dataset, against the iteration number t . From Fig. 3 (left) and (middle), we observe that the DSGD-GD scheme converges to the Multi-PS solution and reaches consensus under various settings of ϵ_{avg} , at the rates $\mathcal{O}(1/t)$, $\mathcal{O}(1/t^2)$, respectively. In Fig. 3 (right), we evaluate the performance of the trained classifier θ_i^t on the testing dataset with shifted distribution due to θ_i^t . We compare with a non-performatively trained solution obtained by solving $\theta^* = \arg \min_{\theta} \sum_{i=1}^n f_i(\theta; \mathbf{0})$ (DSGD in the legend), i.e., without any shift in distributions, but evaluate the performance on distribution shifted by θ^* . As observed, the test accuracy decreases as sensitivity ϵ_{avg} increases, and DSGD-GD achieves better accuracy than DSGD.

Conclusions & Limitations. In this paper, we studied the Multi-PfD problem, and analyzed its stability when a DSGD-GD scheme is applied. Our results indicate that when agents are *consensus seeking*, Multi-PfD admits a performative stable solution with laxer condition and DSGD-GD achieves linear speedup. Limitations to our current results include the requirement of synchronous updates among agents, strongly convex loss [cf. A1], etc., which shall be explored in future extensions.

References

- B. Le Bars, A. Bellet, M. Tommasi, and AM. Kermarrec. Yes, topology matters in decentralized optimization: Refined convergence and topology learning under heterogeneous data. *arXiv preprint arxiv:2204.04452*, 2022. URL <https://arxiv.org/abs/2204.04452>.
- Pascal Bianchi and Jérémie Jakubowicz. Convergence of a multi-agent projected stochastic gradient algorithm for non-convex optimization. *IEEE transactions on automatic control*, 58(2):391–405, 2012.
- Stephen Boyd, Persi Diaconis, and Lin Xiao. Fastest mixing markov chain on a graph. *SIAM review*, 46(4): 667–689, 2004.
- Gavin Brown, Shlomi Hod, and Iden Kalemaj. Performative prediction in a stateful world. In *AISTATS*, 2022.
- Sebastian Caldas, Sai Meher Karthik Duddu, Peter Wu, Tian Li, Jakub Konečný, H. Brendan McMahan, Virginia Smith, and Ameet Talwalkar. Leaf: A benchmark for federated settings. In *NeurIPS Workshop on Federated Learning for Data Privacy and Confidentiality*, 2019.
- Tianyi Chen, Kaiqing Zhang, Georgios B Giannakis, and Tamer Basar. Communication-efficient policy gradient methods for distributed reinforcement learning. *IEEE Transactions on Control of Network Systems*, 2021.
- Jinshuo Dong, Aaron Roth, Zachary Schutzman, Bo Waggoner, and Zhiwei Steven Wu. Strategic classification from revealed preferences. In *Proceedings of the 2018 ACM Conference on Economics and Computation*, pages 55–70, 2018.
- Dmitriy Drusvyatskiy and Lin Xiao. Stochastic optimization with decision-dependent distributions. *ArXiv preprint arxiv:2011.11173*, 2020.
- Andrzej Granas and James Dugundji. *Fixed point theory*, volume 14. Springer, 2003.
- Moritz Hardt, Nimrod Megiddo, Christos Papadimitriou, and Mary Wootters. Strategic classification. In *ITCS*, page 111–122, 2016.
- Reeber Hopkins, Mark. Spambase. UCI Machine Learning Repository, 1999.
- Zachary Izzo, Lexing Ying, and James Zou. How to learn when data reacts to your model: performative gradient descent. In *ICML*, pages 4641–4650. PMLR, 2021.
- Zachary Izzo, James Zou, and Lexing Ying. How to learn when data gradually reacts to your model. In *AISTATS*, 2022.
- Belhal Karimi, Blazej Miasojedow, Eric Moulines, and Hoi-To Wai. Non-asymptotic analysis of biased stochastic approximation scheme. In *Conference on Learning Theory*, pages 1944–1974. PMLR, 2019.
- Jon Kleinberg and Manish Raghavan. How do classifiers induce agents to invest effort strategically? *ACM Transactions on Economics and Computation (TEAC)*, 8(4):1–23, 2020.
- Anastasia Koloskova, Sebastian Stich, and Martin Jaggi. Decentralized stochastic optimization and gossip algorithms with compressed communication. In *International Conference on Machine Learning*, pages 3478–3487. PMLR, 2019.
- Lingjing Kong, Tao Lin, Anastasia Koloskova, Martin Jaggi, and Sebastian Stich. Consensus control for decentralized deep learning. In *International Conference on Machine Learning*, pages 5686–5696. PMLR, 2021.

- Guanghui Lan, Soomin Lee, and Yi Zhou. Communication-efficient algorithms for decentralized and stochastic optimization. *Mathematical Programming*, 180(1):237–284, 2020.
- Qiang Li and Hoi-To Wai. State dependent performative prediction with stochastic approximation. In *AISTATS*, 2022.
- Xiangru Lian, Ce Zhang, Huan Zhang, Cho-Jui Hsieh, Wei Zhang, and Ji Liu. Can decentralized algorithms outperform centralized algorithms? a case study for decentralized parallel stochastic gradient descent. In *NeurIPS*, 2017.
- Celestine Mendler-Dünger, Juan Perdomo, Tijana Zrnic, and Moritz Hardt. Stochastic optimization for performative prediction. *Advances in Neural Information Processing Systems*, 33:4929–4939, 2020.
- John Miller, Juan C. Perdomo, and Tijana Zrnic. Outside the echo chamber: Optimizing the performative risk. In *ICML*, 2021.
- Eric Moulines and Francis Bach. Non-asymptotic analysis of stochastic approximation algorithms for machine learning. In *Advances in neural information processing systems*, volume 24, 2011.
- Adhyyan Narang, Evan Faulkner, Dmitriy Drusvyatskiy, Maryam Fazel, and Lillian J. Ratliff. Multiplayer performative prediction: Learning in decision-dependent games. In *AISTATS*, 2022.
- Juan Perdomo, Tijana Zrnic, Celestine Mendler-Dünger, and Moritz Hardt. Performative prediction. In *International Conference on Machine Learning*, pages 7599–7609. PMLR, 2020.
- Georgios Piliouras and Fang-Yi Yu. Multi-agent performative prediction: From global stability and optimality to chaos. *arXiv preprint arXiv:2201.10483*, 2022.
- Shi Pu, Alexander Olshevsky, and Ioannis Ch Paschalidis. A sharp estimate on the transient time of distributed stochastic gradient descent. *IEEE Transactions on Automatic Control*, 2021.
- Joaquin Quiñonero-Candela, Masashi Sugiyama, Anton Schwaighofer, and Neil D Lawrence. *Dataset shift in machine learning*. MIT Press, 2008.
- S Sundhar Ram, Angelia Nedić, and Venugopal V Veeravalli. Distributed stochastic subgradient projection algorithms for convex optimization. *Journal of optimization theory and applications*, 147(3):516–545, 2010.
- Mitas Ray, Lillian J Ratliff, Dmitriy Drusvyatskiy, and Maryam Fazel. Decision-dependent risk minimization in geometrically decaying dynamic environments. In *AAAI Conference on Artificial Intelligence, To appear*, 2022.
- Ali H Sayed. Adaptation, learning, and optimization over networks. *Foundations and Trends in Machine Learning*, 7:311–801, 2014.
- Hanlin Tang, Xiangru Lian, Ming Yan, Ce Zhang, and Ji Liu. d^2 : Decentralized training over decentralized data. In *International Conference on Machine Learning*, pages 4848–4856. PMLR, 2018.
- Killian Wood, Gianluca Bianchin, and Emiliano Dall’Anese. Online projected gradient descent for stochastic optimization with decision-dependent distributions. *IEEE Control Systems Letters*, 6:1646–1651, 2021.
- Kun Yuan and Sulaiman A Alghunaim. Removing data heterogeneity influence enhances network topology dependence of decentralized sgd. *arXiv preprint arXiv:2105.08023*, 2021.
- Kaiqing Zhang, Zhuoran Yang, Han Liu, Tong Zhang, and Tamer Basar. Fully decentralized multi-agent reinforcement learning with networked agents. In *International Conference on Machine Learning*, pages 5872–5881. PMLR, 2018.

Kaiqing Zhang, Alec Koppel, Hao Zhu, and Tamer Başar. Global convergence of policy gradient methods to (almost) locally optimal policies. *SIAM Journal on Control and Optimization*, 58(6):3586–3612, 2020.

Kaiqing Zhang, Zhuoran Yang, and Tamer Başar. Multi-agent reinforcement learning: A selective overview of theories and algorithms. *Handbook of Reinforcement Learning and Control*, pages 321–384, 2021.

Tijana Zrnic, Eric Mazumdar, Shankar Sastry, and Michael Jordan. Who leads and who follows in strategic classification? In *NeurIPS*, volume 34, 2021.

A Proof of Proposition 1

Fix any $\theta', \theta \in \mathbb{R}^d$. The optimality condition to (11) implies that

$$\sum_{i=1}^n \nabla f_i(\mathcal{M}(\theta); \theta) = \mathbf{0}, \quad \sum_{i=1}^n \nabla f_i(\mathcal{M}(\theta'); \theta') = \mathbf{0}. \quad (29)$$

Note that the gradients are taken w.r.t. the first argument in the function f_i . Observe the chain

$$0 = \langle \mathbf{0} | \mathcal{M}(\theta) - \mathcal{M}(\theta') \rangle = \left\langle \sum_{i=1}^n [\nabla f_i(\mathcal{M}(\theta); \theta) - \nabla f_i(\mathcal{M}(\theta'); \theta')] | \mathcal{M}(\theta) - \mathcal{M}(\theta') \right\rangle.$$

Adding and subtracting $\sum_{i=1}^n \nabla f_i(\mathcal{M}(\theta); \theta')$ implies the equality:

$$\begin{aligned} & \sum_{i=1}^n \langle \nabla f_i(\mathcal{M}(\theta); \theta') - \nabla f_i(\mathcal{M}(\theta); \theta) | \mathcal{M}(\theta) - \mathcal{M}(\theta') \rangle \\ & = \sum_{i=1}^n \langle (\nabla f_i(\mathcal{M}(\theta); \theta') - \nabla f_i(\mathcal{M}(\theta'); \theta')) | \mathcal{M}(\theta) - \mathcal{M}(\theta') \rangle. \end{aligned} \quad (30)$$

Applying A1 to the right hand side of (30) lead to:

$$\sum_{i=1}^n \langle (\nabla f_i(\mathcal{M}(\theta); \theta') - \nabla f_i(\mathcal{M}(\theta'); \theta')) | \mathcal{M}(\theta) - \mathcal{M}(\theta') \rangle \geq n\mu \|\mathcal{M}(\theta) - \mathcal{M}(\theta')\|^2.$$

Meanwhile, applying Lemma 2 to the left hand side of (30) gives

$$\begin{aligned} & \sum_{i=1}^n \langle \nabla f_i(\mathcal{M}(\theta); \theta') - \nabla f_i(\mathcal{M}(\theta); \theta) | \mathcal{M}(\theta) - \mathcal{M}(\theta') \rangle \\ & \leq \sum_{i=1}^n \epsilon_i L \|\theta' - \theta\| \|\mathcal{M}(\theta) - \mathcal{M}(\theta')\|. \end{aligned}$$

Substituting back into (30) implies that

$$\|\mathcal{M}(\theta) - \mathcal{M}(\theta')\| \leq \frac{\sum_{i=1}^n \epsilon_i L}{n\mu} \|\theta - \theta'\| = \frac{\epsilon_{\text{avg}} L}{\mu} \|\theta - \theta'\|. \quad (31)$$

Therefore, the map $\mathcal{M} : \mathbb{R}^d \rightarrow \mathbb{R}^d$ is a contraction if $\epsilon_{\text{avg}} < \mu/L$. Subsequently, by the Banach fixed point theorem [Granas and Dugundji, 2003], the map $\mathcal{M}(\theta)$ admits a unique fixed point which is denoted as θ^{PS} .

To prove the converse, we consider the following instantiation of (11) with

$$\ell(\theta; Z) = \frac{1}{2}(\theta - Z)^2, \quad Z \sim \mathcal{D}_i(\theta) \iff Z \sim \mathcal{N}(\mu_i + \epsilon_i \theta, 1) \quad (32)$$

Note that the above satisfies A1 with $\mu = 1$, A2 with $L = 1$, A3 with ϵ_i for $i = 1, \dots, n$. We consider a case where it holds $\epsilon_{\text{avg}} \geq \mu/L = 1$. We also let $\mu_{\text{avg}} := (1/n) \sum_{i=1}^n \mu_i \neq 0$.

We observe

$$\begin{aligned} f_i(\theta'; \theta) & = \mathbb{E}_{Z \sim \mathcal{D}_i(\theta)} \left[\frac{1}{2}(\theta' - Z)^2 \right] = \mathbb{E}_{\tilde{Z} \sim \mathcal{N}(0,1)} \left[\frac{1}{2}(\theta' - \mu_i - \epsilon_i \theta - \tilde{Z})^2 \right] \\ & = \frac{1}{2}(\theta' - \mu_i - \epsilon_i \theta)^2 + \frac{1}{2}. \end{aligned} \quad (33)$$

For any $\theta \in \mathbb{R}$, it can be shown that

$$\mathcal{M}(\theta) = \arg \min_{\theta' \in \mathbb{R}} \frac{1}{2n} \sum_{i=1}^n (\theta' - \mu_i - \epsilon_i \theta)^2 = \epsilon_{\text{avg}} \theta + \mu_{\text{avg}} \quad (34)$$

Thus, applying the map for T times leads to

$$\mathcal{M}^T(\theta) = \epsilon_{\text{avg}}^T \theta + (1 + \epsilon_{\text{avg}} + \dots + \epsilon_{\text{avg}}^{T-1}) \mu_{\text{avg}} \quad (35)$$

Since $\epsilon_{\text{avg}} > 1$ and $\mu_{\text{avg}} \neq 0$, we have $\lim_{T \rightarrow \infty} |\mathcal{M}^T(\theta)| = \infty$ and the map is not a contraction.

B Proof of Lemma 3

Recall that $\tilde{\boldsymbol{\theta}}^t := \bar{\boldsymbol{\theta}}^t - \boldsymbol{\theta}^{PS}$ is the error of averaged decision at the t th iteration. Using (21), we have

$$\left\| \tilde{\boldsymbol{\theta}}^{t+1} \right\|^2 = \left\| \tilde{\boldsymbol{\theta}}^t \right\|^2 - \frac{2\gamma_{t+1}}{n} \left\langle \tilde{\boldsymbol{\theta}}^t \mid \sum_{i=1}^n \nabla \ell(\boldsymbol{\theta}_i^t; Z_i^{t+1}) \right\rangle + \frac{\gamma_{t+1}^2}{n^2} \left\| \sum_{i=1}^n \nabla \ell(\boldsymbol{\theta}_i^t; Z_i^{t+1}) \right\|^2. \quad (36)$$

We consider taking the conditional expectation $\mathbb{E}_t[\cdot]$ on the both sides. Using the fixed point condition $\sum_{i=1}^n \nabla f_i(\boldsymbol{\theta}^{PS}; \boldsymbol{\theta}^{PS}) = \mathbf{0}$, we observe the following equivalent expression for the last term

$$\left\| \sum_{i=1}^n \nabla \ell(\boldsymbol{\theta}_i^t; Z_i^{t+1}) \right\|^2 = \left\| \sum_{i=1}^n [\nabla \ell(\boldsymbol{\theta}_i^t; Z_i^{t+1}) - \nabla f_i(\boldsymbol{\theta}_i^t; \boldsymbol{\theta}_i^t) + \nabla f_i(\boldsymbol{\theta}_i^t; \boldsymbol{\theta}_i^t) - \nabla f_i(\boldsymbol{\theta}^{PS}; \boldsymbol{\theta}^{PS})] \right\|^2$$

Observe that Z_i^{t+1} , $i = 1, \dots, n$ are independent r.v.s, taking the conditional expectation $\mathbb{E}_t[\cdot]$ yields the upper bound to the above term

$$\begin{aligned} & \mathbb{E}_t \left\| \sum_{i=1}^n \nabla \ell(\boldsymbol{\theta}_i^t; Z_i^{t+1}) \right\|^2 \\ & \leq 2 \sum_{i=1}^n \mathbb{E}_t \left\| \nabla \ell(\boldsymbol{\theta}_i^t; Z_i^{t+1}) - \nabla f_i(\boldsymbol{\theta}_i^t; \boldsymbol{\theta}_i^t) \right\|^2 + 2n \sum_{i=1}^n \left\| \nabla f_i(\boldsymbol{\theta}_i^t; \boldsymbol{\theta}_i^t) - \nabla f_i(\boldsymbol{\theta}^{PS}; \boldsymbol{\theta}^{PS}) \right\|^2 \\ & \leq 2 \sum_{i=1}^n \sigma^2 (1 + \|\boldsymbol{\theta}_i^t - \boldsymbol{\theta}^{PS}\|^2) + 2n \sum_{i=1}^n L^2 (1 + \epsilon_i)^2 \|\boldsymbol{\theta}_i^t - \boldsymbol{\theta}^{PS}\|^2 \\ & \leq 2\sigma^2 n + 4n[\sigma^2 + nL^2(1 + \epsilon_{\max})^2] \left\| \tilde{\boldsymbol{\theta}}^t \right\|^2 + 4[\sigma^2 + nL^2(1 + \epsilon_{\max})^2] \left\| \boldsymbol{\Theta}_o^t \right\|_F^2 \end{aligned} \quad (37)$$

where the first inequality is due to A5 and Lemma 2. We conclude that

$$\frac{1}{n^2} \mathbb{E}_t \left\| \sum_{i=1}^n \nabla \ell(\boldsymbol{\theta}_i^t; Z_i^{t+1}) \right\|^2 \leq \frac{2\sigma^2}{n} + c_2 \left\| \tilde{\boldsymbol{\theta}}^t \right\|^2 + c_2 \frac{1}{n} \left\| \boldsymbol{\Theta}_o^t \right\|_F^2 \quad (38)$$

where we recall the definition that $c_2 = 4 \left(\frac{\sigma^2}{n} + L^2(1 + \epsilon_{\max})^2 \right)$.

Next, we focus on the inner product term in (36), we have

$$\begin{aligned} \left\langle \tilde{\boldsymbol{\theta}}^t \mid \sum_{i=1}^n \nabla f_i(\boldsymbol{\theta}_i^t; \boldsymbol{\theta}_i^t) \right\rangle &= \sum_{i=1}^n \left\langle \tilde{\boldsymbol{\theta}}^t \mid \nabla f_i(\boldsymbol{\theta}_i^t; \boldsymbol{\theta}_i^t) - \nabla f_i(\bar{\boldsymbol{\theta}}^t; \boldsymbol{\theta}^{PS}) \right\rangle \\ &+ \sum_{i=1}^n \left\langle \tilde{\boldsymbol{\theta}}^t \mid \nabla f_i(\bar{\boldsymbol{\theta}}^t; \boldsymbol{\theta}^{PS}) - \nabla f_i(\boldsymbol{\theta}^{PS}; \boldsymbol{\theta}^{PS}) \right\rangle \end{aligned} \quad (39)$$

Applying the Cauchy-Schwarz inequality and A2, A3, we obtain

$$\begin{aligned} \sum_{i=1}^n \left\langle \tilde{\boldsymbol{\theta}}^t \mid \nabla f_i(\boldsymbol{\theta}_i^t; \boldsymbol{\theta}_i^t) - \nabla f_i(\bar{\boldsymbol{\theta}}^t; \boldsymbol{\theta}^{PS}) \right\rangle &\geq - \left\| \tilde{\boldsymbol{\theta}}^t \right\| \sum_{i=1}^n \left(L \left\| \boldsymbol{\theta}_i^t - \bar{\boldsymbol{\theta}}^t \right\| + L\epsilon_i \left\| \boldsymbol{\theta}_i^t - \boldsymbol{\theta}^{PS} \right\| \right) \\ &\geq - \left\| \tilde{\boldsymbol{\theta}}^t \right\| \sum_{i=1}^n \left(L(1 + \epsilon_i) \left\| \boldsymbol{\theta}_i^t - \bar{\boldsymbol{\theta}}^t \right\| + L\epsilon_i \left\| \tilde{\boldsymbol{\theta}}^t \right\| \right). \end{aligned} \quad (40)$$

Meanwhile, using the strong convexity property of $\ell(\cdot; \cdot)$ [cf. A1], we have

$$\sum_{i=1}^n \left\langle \tilde{\boldsymbol{\theta}}^t \mid \nabla f_i(\bar{\boldsymbol{\theta}}^t; \boldsymbol{\theta}^{PS}) - \nabla f_i(\boldsymbol{\theta}^{PS}; \boldsymbol{\theta}^{PS}) \right\rangle \geq n\mu \left\| \tilde{\boldsymbol{\theta}}^t \right\|^2. \quad (41)$$

Summing up the two lower bounds and rearranging terms give

$$\frac{1}{n} \mathbb{E}_t \left\langle \tilde{\boldsymbol{\theta}}^t \mid \sum_{i=1}^n \nabla f_i(\boldsymbol{\theta}_i^t, \boldsymbol{\theta}_i^t) \right\rangle \geq (\mu - L\epsilon_{\text{avg}}) \|\tilde{\boldsymbol{\theta}}^t\|^2 - \frac{L}{n} (1 + \epsilon_{\text{max}}) \sum_{i=1}^n \|\tilde{\boldsymbol{\theta}}^t\| \|\boldsymbol{\theta}_i^t - \bar{\boldsymbol{\theta}}^t\|. \quad (42)$$

For any $\alpha > 0$, using the Young's inequality shows that the above can be further lower bounded by

$$\begin{aligned} & \left[\mu - L\epsilon_{\text{avg}} - \frac{\alpha}{2n} L(1 + \epsilon_{\text{max}}) \right] \|\tilde{\boldsymbol{\theta}}^t\|^2 - \frac{L(1 + \epsilon_{\text{max}})}{2n\alpha} \sum_{i=1}^n \|\boldsymbol{\theta}_i^t - \bar{\boldsymbol{\theta}}^t\|^2 \\ & \geq \left[\mu - L\epsilon_{\text{avg}} - \frac{\alpha}{2n} L(1 + \epsilon_{\text{max}}) \right] \|\tilde{\boldsymbol{\theta}}^t\|^2 - \frac{L(1 + \epsilon_{\text{max}})}{2n\alpha} \|\boldsymbol{\Theta}_o^t\|_F^2 \\ & \geq [\mu - (1 + \delta)L\epsilon_{\text{avg}}] \|\tilde{\boldsymbol{\theta}}^t\|^2 - \frac{L(1 + \epsilon_{\text{max}})^2}{4n^2\delta\epsilon_{\text{avg}}} \|\boldsymbol{\Theta}_o^t\|_F^2, \end{aligned} \quad (43)$$

where we have set $\alpha = \frac{2n\delta\epsilon_{\text{avg}}}{1 + \epsilon_{\text{max}}}$ to yield the last inequality.

Substituting (38), (43) back to the inequality (36) gives us the desired result. In particular,

$$\begin{aligned} \mathbb{E}_t \|\tilde{\boldsymbol{\theta}}^{t+1}\|^2 & \leq \|\tilde{\boldsymbol{\theta}}^t\|^2 - 2\gamma_{t+1} \left[[\mu - (1 + \delta)L\epsilon_{\text{avg}}] \|\tilde{\boldsymbol{\theta}}^t\|^2 - \frac{L(1 + \epsilon_{\text{max}})^2}{4n^2\delta\epsilon_{\text{avg}}} \|\boldsymbol{\Theta}_o^t\|_F^2 \right] \\ & \quad + \gamma_{t+1}^2 \left[\frac{2\sigma^2}{n} + c_2 \|\tilde{\boldsymbol{\theta}}^t\|^2 + c_2 \frac{1}{n} \|\boldsymbol{\Theta}_o^t\|_F^2 \right] \\ & = (1 - 2\tilde{\mu}\gamma_{t+1} + c_2\gamma_{t+1}^2) \|\tilde{\boldsymbol{\theta}}^t\|^2 + \left[c_1 \frac{\gamma_{t+1}}{n} + c_2 \frac{\gamma_{t+1}^2}{n} \right] \|\boldsymbol{\Theta}_o^t\|_F^2 + \frac{2\sigma^2}{n} \gamma_{t+1}^2 \\ & \leq (1 - \tilde{\mu}\gamma_{t+1}) \|\tilde{\boldsymbol{\theta}}^t\|^2 + \left[c_1 \frac{\gamma_{t+1}}{n} + c_2 \frac{\gamma_{t+1}^2}{n} \right] \|\boldsymbol{\Theta}_o^t\|_F^2 + \frac{2\sigma^2}{n} \gamma_{t+1}^2 \end{aligned} \quad (44)$$

where we recall the constants $c_1 := \frac{L(1 + \epsilon_{\text{max}})^2}{2n\delta\epsilon_{\text{avg}}}$, $c_2 := 4 \left(\frac{\sigma^2}{n} + L^2(1 + \epsilon_{\text{max}})^2 \right)$ and $\tilde{\mu} := \mu - (1 + \delta)\epsilon_{\text{avg}}L$ and the last inequality is obtained by observing the condition $\gamma_{t+1} \leq \tilde{\mu}/c_2$.

C Proof of Lemma 4

To simplify notations, we denote

$$\begin{aligned} \tilde{\nabla} F^t & := (\nabla \ell(\boldsymbol{\theta}_1^t; Z_1^{t+1}), \dots, \nabla \ell(\boldsymbol{\theta}_n^t; Z_n^{t+1}))^\top \in \mathbb{R}^{n \times d}, \\ \boldsymbol{\Theta}^t & := (\boldsymbol{\theta}_1^t, \dots, \boldsymbol{\theta}_n^t)^\top \in \mathbb{R}^{n \times d}, \quad \bar{\boldsymbol{\Theta}}^t := (1/n)\mathbf{1}\mathbf{1}^\top \boldsymbol{\Theta}^t \in \mathbb{R}^n. \end{aligned} \quad (45)$$

Notice that $\boldsymbol{\Theta}_o^t = \boldsymbol{\Theta}^t - \bar{\boldsymbol{\Theta}}^t = (\mathbf{I} - (1/n)\mathbf{1}\mathbf{1}^\top) \boldsymbol{\Theta}^t$. We first observe the following relation:

$$\begin{aligned} \boldsymbol{\Theta}_o^{t+1} & = \boldsymbol{\Theta}^{t+1} - \bar{\boldsymbol{\Theta}}^{t+1} = \left(\mathbf{I} - \frac{1}{n} \mathbf{1}\mathbf{1}^\top \right) \boldsymbol{\Theta}^{t+1} = \left(\mathbf{I} - \frac{1}{n} \mathbf{1}\mathbf{1}^\top \right) (\mathbf{W}\boldsymbol{\Theta}^t - \gamma_{t+1} \tilde{\nabla} F^t) \\ & = \left(\mathbf{W} - \frac{1}{n} \mathbf{1}\mathbf{1}^\top \right) \boldsymbol{\Theta}_o^t - \gamma_{t+1} \left(\mathbf{I} - \frac{1}{n} \mathbf{1}\mathbf{1}^\top \right) \tilde{\nabla} F^t, \end{aligned}$$

where the last equality is due to $(\mathbf{I} - (1/n)\mathbf{1}\mathbf{1}^\top)\mathbf{W} = (\mathbf{W} - (1/n)\mathbf{1}\mathbf{1}^\top)(\mathbf{I} - (1/n)\mathbf{1}\mathbf{1}^\top)$ as \mathbf{W} is a doubly stochastic matrix.

Computing the squared norm of the consensus error leads to: for any $\alpha > 0$,

$$\begin{aligned} \mathbb{E}_t \|\boldsymbol{\Theta}_o^{t+1}\|_F^2 & \leq (1 + \alpha)(1 - \rho)^2 \|\boldsymbol{\Theta}_o^t\|_F^2 + (1 + \frac{1}{\alpha})\gamma_{t+1}^2 \mathbb{E}_t \left\| \left(\mathbf{I} - \frac{1}{n} \mathbf{1}\mathbf{1}^\top \right) \tilde{\nabla} F^t \right\|_F^2 \\ & \leq (1 - \rho) \|\boldsymbol{\Theta}_o^t\|_F^2 + \frac{\gamma_{t+1}^2}{\rho} \mathbb{E}_t \left\| \left(\mathbf{I} - \frac{1}{n} \mathbf{1}\mathbf{1}^\top \right) \tilde{\nabla} F^t \right\|_F^2, \end{aligned} \quad (46)$$

where we have applied A4 in the first inequality and set $\alpha = \frac{\rho}{1-\rho}$ in the second inequality. The last term in the above inequality can be bounded as

$$\begin{aligned}
\mathbb{E}_t \left\| \left(\mathbf{I} - \frac{1}{n} \mathbf{1}\mathbf{1}^\top \right) \tilde{\nabla} F^t \right\|_F^2 &= \mathbb{E}_t \left[\sum_{i=1}^n \left\| \nabla \ell(\boldsymbol{\theta}_i^t; Z_i^{t+1}) - \frac{1}{n} \sum_{j=1}^n \nabla \ell(\boldsymbol{\theta}_j^t; Z_j^{t+1}) \right\|^2 \right] \\
&\leq 3 \sum_{i=1}^n \mathbb{E}_t \left\| \nabla \ell(\boldsymbol{\theta}_i^t; Z_i^{t+1}) - \nabla f_i(\boldsymbol{\theta}_i^t, \boldsymbol{\theta}_i^t) \right\|^2 + \frac{3}{n} \sum_{j=1}^n \mathbb{E}_t \left\| \nabla \ell(\boldsymbol{\theta}_j^t; Z_j^{t+1}) - \nabla f_j(\boldsymbol{\theta}_j^t, \boldsymbol{\theta}_j^t) \right\|^2 \\
&\quad + 3 \sum_{i=1}^n \left\| \nabla f_i(\boldsymbol{\theta}_i^t, \boldsymbol{\theta}_i^t) - \frac{1}{n} \sum_{j=1}^n \nabla f_j(\boldsymbol{\theta}_j^t, \boldsymbol{\theta}_j^t) \right\|^2 \\
&\leq 6\sigma^2 \left(n + \sum_{i=1}^n \|\boldsymbol{\theta}_i^t - \boldsymbol{\theta}^{PS}\|^2 \right) + 3 \sum_{i=1}^n \left\| \nabla f_i(\boldsymbol{\theta}_i^t, \boldsymbol{\theta}_i^t) - \frac{1}{n} \sum_{j=1}^n \nabla f_j(\boldsymbol{\theta}_j^t, \boldsymbol{\theta}_j^t) \right\|^2 \\
&\leq 6\sigma^2 \left(n + 2n \|\tilde{\boldsymbol{\theta}}^t\|^2 + 2 \|\boldsymbol{\Theta}_o^t\|_F^2 \right) + 3 \sum_{i=1}^n \left\| \nabla f_i(\boldsymbol{\theta}_i^t, \boldsymbol{\theta}_i^t) - \frac{1}{n} \sum_{j=1}^n \nabla f_j(\boldsymbol{\theta}_j^t, \boldsymbol{\theta}_j^t) \right\|^2
\end{aligned} \tag{47}$$

where the second last inequality is due to A5. For each $i = 1, \dots, n$, we observe

$$\begin{aligned}
&\left\| \nabla f_i(\boldsymbol{\theta}_i^t, \boldsymbol{\theta}_i^t) - \nabla f_i(\bar{\boldsymbol{\theta}}^t, \bar{\boldsymbol{\theta}}^t) + \nabla f_i(\bar{\boldsymbol{\theta}}^t, \bar{\boldsymbol{\theta}}^t) - \frac{1}{n} \sum_{j=1}^n \nabla f_j(\bar{\boldsymbol{\theta}}^t, \bar{\boldsymbol{\theta}}^t) - \frac{1}{n} \sum_{j=1}^n [\nabla f_j(\boldsymbol{\theta}_j^t, \boldsymbol{\theta}_j^t) - \nabla f_j(\bar{\boldsymbol{\theta}}^t, \bar{\boldsymbol{\theta}}^t)] \right\|^2 \\
&\leq 3 \left\| \nabla f_i(\boldsymbol{\theta}_i^t, \boldsymbol{\theta}_i^t) - \nabla f_i(\bar{\boldsymbol{\theta}}^t, \bar{\boldsymbol{\theta}}^t) \right\|^2 + 3 \left\| \nabla f_i(\bar{\boldsymbol{\theta}}^t, \bar{\boldsymbol{\theta}}^t) - \frac{1}{n} \sum_{j=1}^n \nabla f_j(\bar{\boldsymbol{\theta}}^t, \bar{\boldsymbol{\theta}}^t) \right\|^2 \\
&\quad + \frac{3}{n} \sum_{j=1}^n \left\| \nabla f_j(\boldsymbol{\theta}_j^t, \boldsymbol{\theta}_j^t) - \nabla f_j(\bar{\boldsymbol{\theta}}^t, \bar{\boldsymbol{\theta}}^t) \right\|^2 \\
&\leq 3 \left\| \nabla f_i(\boldsymbol{\theta}_i^t, \boldsymbol{\theta}_i^t) - \nabla f_i(\bar{\boldsymbol{\theta}}^t, \bar{\boldsymbol{\theta}}^t) \right\|^2 + \frac{3}{n} \sum_{j=1}^n \left\| \nabla f_j(\boldsymbol{\theta}_j^t, \boldsymbol{\theta}_j^t) - \nabla f_j(\bar{\boldsymbol{\theta}}^t, \bar{\boldsymbol{\theta}}^t) \right\|^2 + 3\varsigma^2 \left(1 + \|\tilde{\boldsymbol{\theta}}^t\|^2 \right)
\end{aligned} \tag{48}$$

where the last inequality is due to A6. Now, we observe

$$\begin{aligned}
\sum_{i=1}^n \left\| \nabla f_i(\boldsymbol{\theta}_i^t, \boldsymbol{\theta}_i^t) - \frac{1}{n} \sum_{j=1}^n \nabla f_j(\boldsymbol{\theta}_j^t, \boldsymbol{\theta}_j^t) \right\|^2 &\leq 6 \sum_{i=1}^n \left\| \nabla f_i(\boldsymbol{\theta}_i^t, \boldsymbol{\theta}_i^t) - \nabla f_i(\bar{\boldsymbol{\theta}}^t, \bar{\boldsymbol{\theta}}^t) \right\|^2 + 3n\varsigma^2 \left(1 + \|\tilde{\boldsymbol{\theta}}^t\|^2 \right) \\
&\leq 6L^2(1 + \epsilon_{\max})^2 \|\boldsymbol{\Theta}_o^t\|_F^2 + 3n\varsigma^2 \left(1 + \|\tilde{\boldsymbol{\theta}}^t\|^2 \right)
\end{aligned}$$

where the second inequality is due to Lemma 2 and the definition of $\boldsymbol{\Theta}_o^t$.

Substituting the above bounds into (47) leads to

$$\begin{aligned}
&\mathbb{E}_t \left\| \left(\mathbf{I} - \frac{1}{n} \mathbf{1}\mathbf{1}^\top \right) \tilde{\nabla} F^t \right\|_F^2 \\
&\leq 6\sigma^2 \left(n + 2n \|\tilde{\boldsymbol{\theta}}^t\|^2 + 2 \|\boldsymbol{\Theta}_o^t\|_F^2 \right) + 18L^2(1 + \epsilon_{\max})^2 \|\boldsymbol{\Theta}_o^t\|_F^2 + 9n\varsigma^2 \left(1 + \|\tilde{\boldsymbol{\theta}}^t\|^2 \right) \\
&\leq 9n[\sigma^2 + \varsigma^2] + 12n[\sigma^2 + \varsigma^2] \|\tilde{\boldsymbol{\theta}}^t\|^2 + [12\sigma^2 + 18L^2(1 + \epsilon_{\max})^2] \|\boldsymbol{\Theta}_o^t\|_F^2
\end{aligned} \tag{49}$$

Let $c_3 := 12\sigma^2 + 18L^2(1 + \epsilon_{\max})^2$. Substituting the above inequality into (46) gives us

$$\begin{aligned} \mathbb{E}_t \|\Theta_o^{t+1}\|_F^2 &\leq (1 - \rho) \|\Theta_o^t\|_F^2 + \frac{\gamma_{t+1}^2}{\rho} \left(12n[\sigma^2 + \varsigma^2] \|\tilde{\theta}^t\|^2 + c_3 \|\Theta_o^t\|_F^2 \right) + 9n(\sigma^2 + \varsigma^2) \frac{\gamma_{t+1}^2}{\rho} \\ &\leq (1 - \rho/2) \|\Theta_o^t\|_F^2 + \frac{\gamma_{t+1}^2}{\rho} 12n[\sigma^2 + \varsigma^2] \|\tilde{\theta}^t\|^2 + 9n(\sigma^2 + \varsigma^2) \frac{\gamma_{t+1}^2}{\rho}, \end{aligned}$$

where the last inequality is due to the step size condition $\gamma_{t+1}^2 \leq \rho^2/2c_3$. The proof is concluded.

Alternative Bound without A6 We consider bounding (48) without using A6. Instead, we only assume that $\max_{i=1, \dots, n} \|\nabla f_i(\theta^{PS}; \theta^{PS})\|^2 \leq \varsigma^2$. We observe

$$\begin{aligned} \left\| \nabla f_i(\bar{\theta}^t, \bar{\theta}^t) - \nabla f(\bar{\theta}^t, \bar{\theta}^t) \right\|^2 &\leq 2 \|\nabla f_i(\theta^{PS}; \theta^{PS})\|^2 \\ &\quad + 2 \left\| \nabla f_i(\bar{\theta}^t, \bar{\theta}^t) - \nabla f_i(\theta^{PS}; \theta^{PS}) + \nabla f(\theta^{PS}; \theta^{PS}) - \nabla f(\bar{\theta}^t, \bar{\theta}^t) \right\|^2 \\ &\leq 2 \|\nabla f_i(\theta^{PS}; \theta^{PS})\|^2 + 8L^2(1 + \epsilon_{\max})^2 \|\tilde{\theta}^t\|^2 \leq 2\varsigma^2 + 8L^2(1 + \epsilon_{\max})^2 \|\tilde{\theta}^t\|^2, \end{aligned} \quad (50)$$

for all $i = 1, \dots, n$. This leads to

$$\begin{aligned} \sum_{i=1}^n \left\| \nabla f_i(\theta_i^t, \theta_i^t) - \frac{1}{n} \sum_{j=1}^n \nabla f_j(\theta_j^t, \theta_j^t) \right\|^2 \\ \leq 6L^2(1 + \epsilon_{\max})^2 \|\Theta_o^t\|_F^2 + 2n\varsigma^2 + 8nL^2(1 + \epsilon_{\max})^2 \|\tilde{\theta}^t\|^2. \end{aligned}$$

Subsequently,

$$\begin{aligned} \mathbb{E}_t \left\| \left(\mathbf{I} - \frac{1}{n} \mathbf{1}\mathbf{1}^\top \right) \tilde{\nabla} F^t \right\|_F^2 \\ \leq 6\sigma^2 \left(n + 2n \|\tilde{\theta}^t\|^2 + 2 \|\Theta_o^t\|_F^2 \right) + 6n\varsigma^2 + 6L^2(1 + \epsilon_{\max})^2 \left(3 \|\Theta_o^t\|_F^2 + 4n \|\tilde{\theta}^t\|^2 \right) \\ = 6n[\sigma^2 + \varsigma^2] + 12n \left[\sigma^2 + 2L^2(1 + \epsilon_{\max})^2 \right] \|\tilde{\theta}^t\|^2 + [12\sigma^2 + 18L^2(1 + \epsilon_{\max})^2] \|\Theta_o^t\|_F^2 \end{aligned} \quad (51)$$

Taking $c_3 := 12\sigma^2 + 18L^2(1 + \epsilon_{\max})^2$ as before and substituting the inequality into (46) yields

$$\begin{aligned} \mathbb{E}_t \|\Theta_o^{t+1}\|_F^2 \\ \leq (1 - \rho) \|\Theta_o^t\|_F^2 + \frac{\gamma_{t+1}^2}{\rho} \left(12n \left[\sigma^2 + 2L^2(1 + \epsilon_{\max})^2 \right] \|\tilde{\theta}^t\|^2 + c_3 \|\Theta_o^t\|_F^2 \right) + 6n(\sigma^2 + \varsigma^2) \frac{\gamma_{t+1}^2}{\rho} \\ \leq (1 - \rho/2) \|\Theta_o^t\|_F^2 + \frac{\gamma_{t+1}^2}{\rho} 12n \left[\sigma^2 + 2L^2(1 + \epsilon_{\max})^2 \right] \|\tilde{\theta}^t\|^2 + 6n(\sigma^2 + \varsigma^2) \frac{\gamma_{t+1}^2}{\rho}, \end{aligned}$$

where the last inequality is due to $\sup_{t \geq 1} \gamma_t \leq \rho/\sqrt{2c_3}$. The above can be simplified into

$$\frac{1}{n} \mathbb{E}_t \|\Theta_o^{t+1}\|_F^2 \leq \left(1 - \frac{\rho}{2} \right) \frac{1}{n} \|\Theta_o^t\|_F^2 + \frac{\gamma_{t+1}^2}{\rho} 12 \left[\sigma^2 + 2L^2(1 + \epsilon_{\max})^2 \right] \|\tilde{\theta}^t\|^2 + 6(\sigma^2 + \varsigma^2) \frac{\gamma_{t+1}^2}{\rho}. \quad (52)$$

Compared to (23), we observe that the above bound entails a larger coefficient for $\|\tilde{\theta}^t\|^2$ which lead to a (slightly) worse convergence bound for the DSGD-GD scheme.

Lastly, we should mention that as in the original Lemma 4, (52) can also be combined with Lemma 3 to develop an alternate version of Lemma 5. Subsequently, we can achieve a similar result as Theorem 1 without assuming A6.

D Proof of Lemma 5

Combining Lemmas 3 and 4 leads to

$$\begin{aligned}
\mathcal{L}_{t+1} &\leq (1 - \tilde{\mu}\gamma_{t+1}) \mathbb{E} \left\| \tilde{\boldsymbol{\theta}}^t \right\|^2 + [c_1\gamma_{t+1} + c_2\gamma_{t+1}^2] \frac{1}{n} \mathbb{E} \left\| \boldsymbol{\Theta}_o^t \right\|_F^2 + \frac{2\sigma^2}{n} \gamma_{t+1}^2 \\
&\quad + \gamma_{t+1} \frac{8c_1}{\rho} \left(\left(1 - \frac{\rho}{2}\right) \frac{1}{n} \mathbb{E} \left\| \boldsymbol{\Theta}_o^t \right\|_F^2 + \frac{\gamma_{t+1}^2}{\rho} 12[\sigma^2 + \varsigma^2] \mathbb{E} \left\| \tilde{\boldsymbol{\theta}}^t \right\|^2 + 9(\sigma^2 + \varsigma^2) \frac{\gamma_{t+1}^2}{\rho} \right) \\
&= \left(1 - \tilde{\mu}\gamma_{t+1} + \frac{96c_1}{\rho^2} [\sigma^2 + \varsigma^2] \gamma_{t+1}^3\right) \mathbb{E} \left\| \tilde{\boldsymbol{\theta}}^t \right\|^2 + \frac{2\sigma^2}{n} \gamma_{t+1}^2 + \frac{72c_1}{\rho^2} (\sigma^2 + \varsigma^2) \gamma_{t+1}^3 \\
&\quad + \gamma_t \frac{8c_1}{\rho} \left(\frac{\gamma_{t+1}}{\gamma_t} \left(1 - \frac{\rho}{2}\right) + \frac{\rho}{8} + \frac{c_2\rho}{8c_1} \gamma_{t+1} \right) \frac{1}{n} \mathbb{E} \left\| \boldsymbol{\Theta}_o^t \right\|_F^2
\end{aligned}$$

Note that by the step size conditions specified in the lemma, we have

$$\begin{aligned}
1 - \tilde{\mu}\gamma_{t+1} + \frac{96c_1}{\rho^2} [\sigma^2 + \varsigma^2] \gamma_{t+1}^3 &\leq 1 - \tilde{\mu}\gamma_{t+1}/2 \\
\frac{\gamma_{t+1}}{\gamma_t} \left(1 - \frac{\rho}{2}\right) + \frac{\rho}{8} + \frac{c_2\rho}{8c_1} \gamma_{t+1} &\leq 1 - \tilde{\mu}\gamma_{t+1}/2.
\end{aligned} \tag{53}$$

Thus, we obtain

$$\mathcal{L}_{t+1} \leq (1 - \tilde{\mu}\gamma_{t+1}/2) \mathcal{L}_t + \frac{2\sigma^2}{n} \gamma_{t+1}^2 + \frac{72c_1}{\rho^2} (\sigma^2 + \varsigma^2) \gamma_{t+1}^3. \tag{54}$$

This concludes the first part of the lemma, i.e., (25). For the second part, we further expand (54) to obtain

$$\begin{aligned}
\mathcal{L}_{t+1} &\leq \prod_{i=1}^{t+1} \left(1 - \frac{\tilde{\mu}\gamma_i}{2}\right) \mathsf{D} + \sum_{s=1}^{t+1} \prod_{i=s+1}^{t+1} (1 - \tilde{\mu}\gamma_i/2) \left(\frac{2\sigma^2}{n} \gamma_s^2 + \frac{72c_1}{\rho^2} (\sigma^2 + \varsigma^2) \gamma_s^3 \right) \\
&\leq \prod_{i=1}^{t+1} \left(1 - \frac{\tilde{\mu}\gamma_i}{2}\right) \mathsf{D} + \frac{288c_1(\sigma^2 + \varsigma^2)}{\rho^2 \tilde{\mu}} \gamma_{t+1}^2 + \frac{8\sigma^2}{\tilde{\mu}n} \gamma_{t+1}.
\end{aligned} \tag{55}$$

where we recall that $\mathsf{D} := \left\| \tilde{\boldsymbol{\theta}}^0 \right\|^2 + \frac{8\gamma_1 c_1}{\rho n} \left\| \boldsymbol{\Theta}_o^0 \right\|_F^2$ and the last inequality is due to Lemma 6 together with the specified step size conditions. The proof is thus concluded.

E Auxilliary Results

Lemma 6. Consider a sequence of non-negative, non-increasing step sizes $\{\gamma_t\}_{t \geq 1}$. Let $a > 0$, $p \in \mathbb{Z}_+$ and $\gamma_1 < 2/a$. If $\gamma_t^p / \gamma_{t+1}^p \leq 1 + (a/2)\gamma_{t+1}^p$ for any $t \geq 1$, then

$$\sum_{j=1}^t \gamma_j^{p+1} \prod_{\ell=j+1}^t (1 - \gamma_\ell a) \leq \frac{2}{a} \gamma_t^p, \quad \forall t \geq 1. \tag{56}$$

Proof. Observe that:

$$\begin{aligned}
\sum_{j=1}^t \gamma_j^{p+1} \prod_{\ell=j+1}^t (1 - \gamma_\ell a) &= \gamma_t^p \sum_{j=1}^t \gamma_j \prod_{\ell=j+1}^t \frac{\gamma_{\ell-1}^p}{\gamma_\ell^p} (1 - \gamma_\ell a) \\
&\stackrel{(a)}{\leq} \gamma_t^p \sum_{j=1}^t \gamma_j \prod_{\ell=j+1}^t \left(1 - \gamma_\ell \frac{a}{2}\right)
\end{aligned}$$

$$\begin{aligned}
&= \frac{2\gamma_t^p}{a} \sum_{j=1}^t \left(\prod_{\ell=j+1}^t (1 - \gamma_\ell a/2) - \prod_{\ell'=j}^t (1 - \gamma_{\ell'} a/2) \right) \\
&= \frac{2\gamma_t^p}{a} \left(1 - \prod_{\ell'=1}^t (1 - \gamma_{\ell'} a/2) \right) \leq \frac{2\gamma_t^p}{a},
\end{aligned}$$

where (a) is due to the following observation

$$\frac{\gamma_{\ell-1}^p}{\gamma_\ell^p} (1 - \gamma_\ell a) \leq \left(1 + \frac{a}{2} \gamma_\ell^p \right) (1 - \gamma_\ell a) \leq 1 - \frac{a}{2} \gamma_\ell.$$

The proof is concluded. \square

Lemma 7. Consider a sequence of non-negative, non-increasing step sizes $\{\gamma_t\}_{t \geq 1}$. Let $p \in \mathbb{Z}^+$. If $\sup_{t \geq 1} \gamma_t^p / \gamma_{t+1}^p \leq 1 + \frac{\rho}{4-2\rho}$, then for any $t \geq 0$, it holds that

$$\sum_{i=1}^{t+1} \left(1 - \frac{\rho}{2} \right)^{t+1-i} \gamma_i^p \leq \frac{4}{\rho} \gamma_{t+1}^p. \quad (57)$$

Proof. We observe the following chain:

$$\begin{aligned}
\sum_{i=1}^{t+1} \left(1 - \frac{\rho}{2} \right)^{t+1-i} \gamma_i^p &= \gamma_{t+1}^p \sum_{i=1}^{t+1} \left(1 - \frac{\rho}{2} \right)^{t+1-i} \left(\frac{\gamma_i}{\gamma_{i+1}} \right)^p \left(\frac{\gamma_{i+1}}{\gamma_{i+2}} \right)^p \cdots \left(\frac{\gamma_t}{\gamma_{t+1}} \right)^p \\
&\leq \gamma_{t+1}^p \sum_{i=1}^{t+1} \left(1 - \frac{\rho}{4} \right)^{t+1-i} \leq \frac{4}{\rho} \gamma_{t+1}^p
\end{aligned}$$

where the second last inequality is due to:

$$\left(1 - \rho/2 \right) \left(\frac{\gamma_{i+1}}{\gamma_{i+2}} \right)^p \leq 1 - \frac{\rho}{4}$$

since $\sup_{k \geq 1} \gamma_{k-1}^p / \gamma_k^p \leq 1 + \frac{\rho}{4-2\rho}$. This completes the proof. \square

F Details of Numerical Experiments and Additional Results

This section provides details for the numerical experiments conducted in §4. We also describe an additional numerical experiment based on the logistic regression Example 1 on synthetic data. The latter examines the effects of heterogeneous data on the convergence rate of DSGD-GD.

For all our experiments, we have performed DSGD-GD with the step size $\gamma_t = a_0 / (a_1 + t)$. Moreover, at each iteration of DSGD-GD, the i th agent draws $\text{batch} \geq 1$ samples from $\mathcal{D}_i(\theta_i^t)$. The parameters $a_0 > 0, a_1 \geq 0, \text{batch} \geq 1$ used for different tasks are specified in Table 1. For both Gaussian mean estimation and `spambase` logistic regression, we use the same parameters for all settings of $\bar{\epsilon} = \epsilon_{\text{avg}}$. We consider using $n = 25$ agents in all experiments, connected on a ring graph. We set the mixing matrix weights as $W_{ij} = 1/3$ for all $(i, j) \in E$, and $W_{ij} = 0$ if $(i, j) \notin E$.

Spam Email Classification. In Fig. 4, we provide additional results for the experiment in the main paper [cf. Fig. 3]. In particular, we compare the training loss $f(\bar{\theta}^t; \bar{\theta}^t)$ and training accuracy against the iteration number t . We also plot the gap to an *approximate* Multi-PS solution in Fig. 4 (right) for $\|\bar{\theta}^t - \theta^{\hat{P}S}\|^2$. Note that the Multi-PS solution compared here is only an approximation obtained by applying a similar method to repeated gradient descent in [Perdomo et al., 2020] on $\min_{\theta} \sum_{i=1}^n f_i(\theta; \theta)$, where we used 1000 gradient descent iterations together with an outer loop of 10^4 deployments. Note that this process is only

Tasks	$\bar{\epsilon} = \epsilon_{\text{avg}}$	a_0	a_1	batch
Gaussian Mean Estimation	see §4	50	10000	1
Spam Email Classification	see §4	50	100000	32
LEAF Synthetic Data (Hetero & Homo)	0.1	200	1000	32
LEAF Synthetic Data (Hetero & Homo)	10.0	1	1000	32

Table 1: Parameters for the numerical experiments.

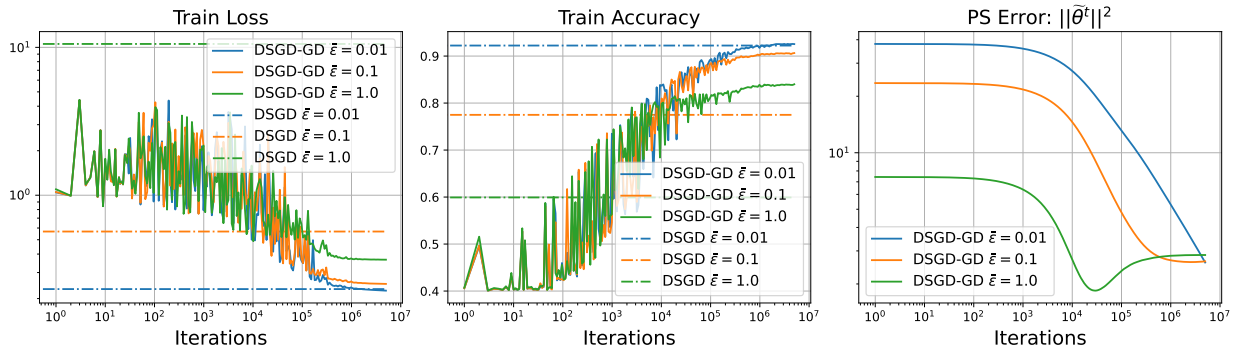


Figure 4: **Additional Results for Spam Email Classification.** (Left) Training Loss. (Middle) Training Accuracy. (Right) Approximate Gap to Multi-PS solution (see below). We also compare the non-performative optimal solution (dashed lines) on the shifted dataset.

guaranteed to find a near-optimal solution, denoted as $\theta^{\hat{P}S}$. Nevertheless, we observe that when the decision dependent distributions becomes more sensitive ($\epsilon_{\text{avg}} = 1$), the DSGD-GD scheme seems unable to reach $\theta^{\hat{P}S}$.

Logistic Regression on LEAF Synthetic Data. To study the effect of homogeneity of data distribution [cf. A6] on the convergence of DSGD-GD, we conduct an additional experiment based on Example 1 but on the LEAF synthetic data [Caldas et al., 2019]. Here, we set the sensitivity parameter at $\epsilon_i = \bar{\epsilon}$ for $i = 1, \dots, 25$ and generate synthetic data using the framework in [Caldas et al., 2019] with the standard deviation $\sigma = 1$ that represents the degree of heterogeneity of the dataset. Note that the framework produces $m_i = 100$ training samples with $d = 100$ features for each agent, denoted as $(\mathbf{X}_k^i, Y_k^i)_{k=1}^{100}$, for $i = 1, \dots, 25$ agents.

We consider two settings and describe them using the notations as in Example 1. In the **heterogeneous** data setting, the base data distribution \mathcal{D}_i^0 for agent i is taken to be $(\mathbf{X}_k^i, Y_k^i)_{k=1}^{100}$ such that $\mathcal{D}_i(\theta) \neq \mathcal{D}_j(\theta)$. In the **homogeneous** data setting, the base data distribution \mathcal{D}_i^0 for agent i is taken to be $((\mathbf{X}_k^i, Y_k^i)_{k=1}^{100})_{i=1}^{25}$, i.e., the entire dataset generated from LEAF. Note that in this case, $\mathcal{D}_i^0 \equiv \mathcal{D}_j^0$ and thus $\mathcal{D}_i(\theta) \equiv \mathcal{D}_j(\theta)$ for any $\theta \in \mathbb{R}^d$ and $i, j = 1, \dots, n$ since $\epsilon_i = \epsilon_{\text{avg}}$. Note that the Multi-PS solution θ^{PS} (if exists) in both settings are unique and identical. Meanwhile, the **homogeneous** case satisfies A6 with $\varsigma = 0$, thus the DSGD-GD scheme applied to it is expected to converge at a faster rate than in the **heterogeneous** case.

Our numerical results are presented in Fig. 5, and we show in Table 1 the simulation parameters. Observe that with $\epsilon_{\text{avg}} = 10$, the local data distributions are too sensitive and the Multi-PS solution θ^{PS} may not exist. With $\epsilon_{\text{avg}} = 0.1$, we observe that the convergence of test accuracy, training loss, etc. are faster with the **homogeneous** case initially. However, as the iteration number t grows, the gap between the **homogeneous** and **heterogeneous** cases fade. This corroborates with our finite-time analysis in (18), where the fluctuation term $\sigma^2 \gamma_t / (n \bar{\mu})$ becomes dominant as $t \gg 1$ in all cases, yet the transient time can be shorter when $\varsigma = 0$ as predicted by (19).

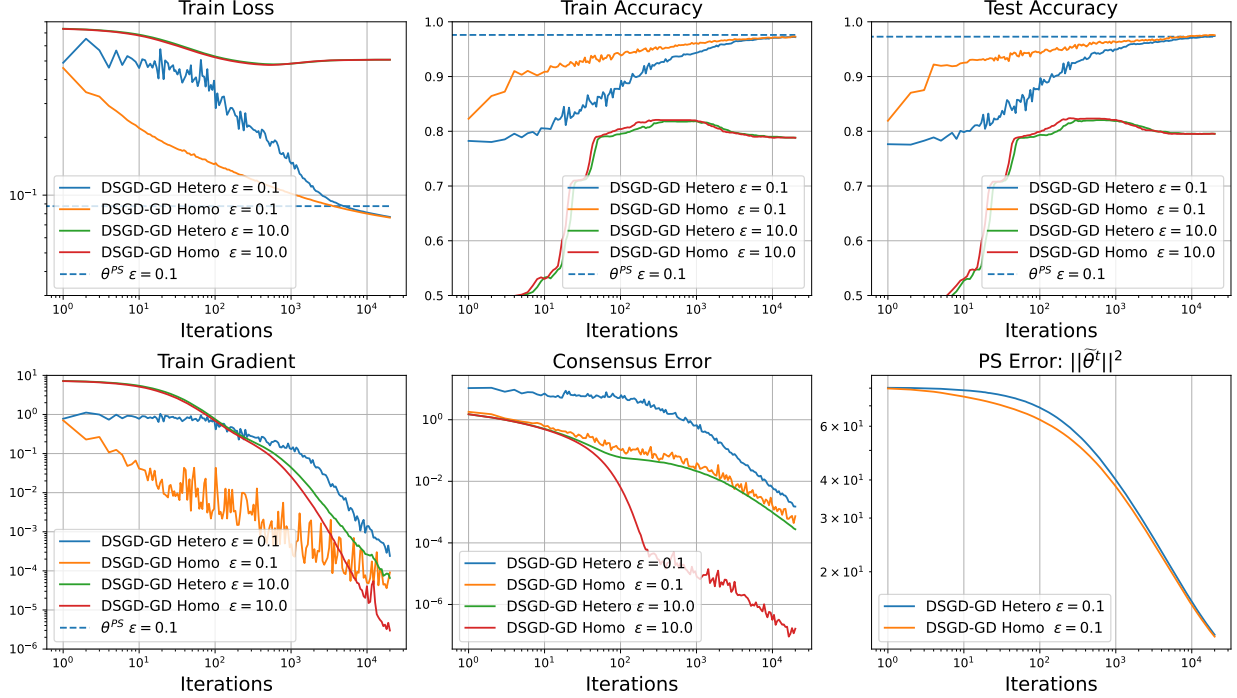


Figure 5: **Logistic Regression on LEAF Synthetic Data.** DSGD-GD in homogeneous and heterogeneous data distribution converge to the same Multi-PS solution.

G Extension to Time-varying Graph

This section shows how to extend our analysis for DSGD-GD to the setting with time-varying communication graph. Let $G^{(t)} = (V, E^{(t)})$ be a simple, undirected graph which is possibly not connected and the graph is associated with a weighted adjacency matrix $\mathbf{W}^{(t)}$. Note that the graph $G^{(t)}$ consists of a fixed set of agents V and a set of time-varying edges $E^{(t)}$.

In lieu of A4, we assume that:

A7. *The time-varying undirected graph sequence $\{G^{(t)}\}_{t \geq 1} = \{(V, E^{(t)})\}_{t \geq 1}$ is B -connected. Specifically, for any $t \geq 1$, there exists a positive integer B such that the undirected graph $(V, E^{(t)} \cup \dots \cup E^{(t+B-1)})$ is connected. For any $t \geq 1$, the mixing matrix $\mathbf{W}^{(t)} \in \mathbb{R}^{n \times n}$ satisfies:*

1. (Topology) $\mathbf{W}_{ij}^{(t)} = 0$ if $(i, j) \notin E^{(t)}$.
2. (Doubly stochastic) $\mathbf{W}^{(t)} \mathbf{1} = (\mathbf{W}^{(t)})^\top \mathbf{1} = \mathbf{1}$.
3. (Fast mixing) Let $\mathbf{A}^{(t)} := \mathbf{W}^{(t)} - \frac{1}{n} \mathbf{1} \mathbf{1}^\top$, there exists $\bar{\rho} \in (0, 1]$ such that $\|\mathbf{A}^{(t+B-1)} \dots \mathbf{A}^{(t)}\|_2 \leq 1 - \bar{\rho}$.

The last condition can be guaranteed under the bounded communication setting, i.e., when the combined graph $(V, E^{(t)} \cup \dots \cup E^{(t+B)})$ is connected for any $t \geq 0$.

Notations. Throughout, we denote $\Theta(m, n) := \mathbb{E}[\|\Theta_o^m\|_F^2 + \dots + \|\Theta_o^n\|_F^2]$ and $\tilde{\theta}(m, n) := \mathbb{E}[\|\tilde{\theta}^m\|^2 + \dots + \|\tilde{\theta}^n\|^2]$, which is the aggregation of consensus error and performative stable gap in one time block whose length is B , respectively.

Proof Sketch. Below we provide a proof sketch for the convergence of DSGD-GD scheme when the latter is applied on a time varying graph satisfying A7. We begin by considering the extensions of Lemmas 3 and 4. As follows,

Lemma 8 (Extension of Lemma 3). Fix any $\delta > 0$ and let $\epsilon_{\text{avg}} \leq \frac{\mu}{(1+\delta)L}$. Under A1, A2, A3, A5 and let the step sizes satisfy $\sup_{t \geq 0} \gamma_{t+1} \leq \frac{\tilde{\mu}}{c_2}$, the following bound holds for any $t \geq 0$,

$$\begin{aligned} \tilde{\boldsymbol{\theta}}(t+1, t+B) &\leq (1 - \tilde{\mu}\gamma_{t+B})^B \tilde{\boldsymbol{\theta}}(t-B+1, t) + \frac{2B\sigma^2}{n} \gamma_{t+1}^2 \\ &\quad + B \left(c_1 \frac{\gamma_{t+1}}{n} + c_2 \frac{\gamma_{t+1}^2}{n} \right) [\boldsymbol{\Theta}(t-B+1, t) + \boldsymbol{\Theta}(t+1, t+B)]. \end{aligned}$$

Proof. Recall the inequality (22) in Lemma 3,

$$\mathbb{E}_t \left\| \tilde{\boldsymbol{\theta}}^{t+1} \right\|^2 \leq (1 - \tilde{\mu}\gamma_{t+1}) \left\| \tilde{\boldsymbol{\theta}}^t \right\|^2 + [c_1 \gamma_{t+1} + c_2 \gamma_{t+1}^2] \frac{1}{n} \left\| \boldsymbol{\Theta}_o^t \right\|_F^2 + \frac{2\sigma^2}{n} \gamma_{t+1}^2. \quad (58)$$

This implies

$$\tilde{\boldsymbol{\theta}}(t+1, t+B) \leq (1 - \tilde{\mu}\gamma_{t+B}) \tilde{\boldsymbol{\theta}}(t, t+B-1) + \left(\frac{c_1 \gamma_{t+1}}{n} + \frac{c_2 \gamma_{t+1}^2}{n} \right) \boldsymbol{\Theta}(t, t+B-1) + \frac{2B\sigma^2}{n} \gamma_{t+1}^2,$$

where we have summed (58) from $t+1$ th to $t+B$ th iteration and noted that the step size γ_t is non-increasing. Applying the above inequality for B times, we can link two consecutive B performative stable gap $\tilde{\boldsymbol{\theta}}(t+1, t+B)$ and $\tilde{\boldsymbol{\theta}}(t-B+1, t)$ by

$$\begin{aligned} \tilde{\boldsymbol{\theta}}(t+1, t+B) &\leq (1 - \tilde{\mu}\gamma_{t+B})^B \tilde{\boldsymbol{\theta}}(t-B+1, t) + \frac{2B\sigma^2}{n} \gamma_{t+1}^2 \\ &\quad + \left(\frac{c_1 \gamma_{t+1}}{n} + \frac{c_2 \gamma_{t+1}^2}{n} \right) [\boldsymbol{\Theta}(t, t+B-1) + \boldsymbol{\Theta}(t-1, t+B-2) + \dots + \boldsymbol{\Theta}(t-B+1, t)]. \end{aligned} \quad (59)$$

For the first term $\boldsymbol{\Theta}(t, t+B-1)$ in the last quantity, we observe the crude bound

$$\boldsymbol{\Theta}(t, t+B-1) \leq \boldsymbol{\Theta}(t+1, t+B) + \mathbb{E} \left\| \boldsymbol{\Theta}_o^t \right\|_F^2 \leq \boldsymbol{\Theta}(t-B+1, t) + \boldsymbol{\Theta}(t+1, t+B).$$

Following the same trick, we get another crude bound as

$$\begin{aligned} &[\boldsymbol{\Theta}(t, t+B-1) + \boldsymbol{\Theta}(t-1, t+B-2) + \dots + \boldsymbol{\Theta}(t-B+1, t)] \\ &\leq B[\boldsymbol{\Theta}(t-B+1, t) + \boldsymbol{\Theta}(t+1, t+B)]. \end{aligned}$$

Substituting back to inequality (59) derives the final bound

$$\begin{aligned} \tilde{\boldsymbol{\theta}}(t+1, t+B) &\leq (1 - \tilde{\mu}\gamma_{t+B})^B \tilde{\boldsymbol{\theta}}(t-B+1, t) + \frac{2B\sigma^2}{n} \gamma_{t+1}^2 \\ &\quad + B \left(c_1 \frac{\gamma_{t+1}}{n} + c_2 \frac{\gamma_{t+1}^2}{n} \right) [\boldsymbol{\Theta}(t-B+1, t) + \boldsymbol{\Theta}(t+1, t+B)]. \end{aligned}$$

□

Lemma 9 (Extension of Lemma 4). Under A2–A5 and A7 and let the step sizes satisfy

$$\sup_{t \geq 0} \gamma_{t+1} \leq \rho / \sqrt{2Bc_3},$$

then it holds for any $t \geq 0$ that

$$\begin{aligned} \boldsymbol{\Theta}(t+1, t+B) &\leq \frac{1 - \bar{\rho}/2}{1 - Bc_3\gamma_{t-B+1}^2/\bar{\rho}} \boldsymbol{\Theta}(t-B+1, t) \\ &\quad + \frac{\gamma_{t-B+1}^2}{\rho - Bc_3\gamma_{t-B+1}^2} \left\{ B^2 d_1 + d_2 B [\tilde{\boldsymbol{\theta}}(t-B+1, t) + \tilde{\boldsymbol{\theta}}(t+1, t+B)] \right\}, \end{aligned} \quad (60)$$

where $d_1 := 9n(\sigma^2 + \varsigma^2)$, $d_2 := 12n(\sigma^2 + \varsigma^2)$.

Proof. Recall the notations (45) and observe that

$$\Theta_o^{t+1} = \Theta^{t+1} - \bar{\Theta}^{t+1} = \underbrace{\left(\mathbf{W}^{t+1} - \frac{1}{n} \mathbf{1}\mathbf{1}^\top \right)}_{=\mathbf{A}^{t+1}} \Theta_o^t - \gamma_{t+1} \left(\mathbf{I} - \frac{1}{n} \mathbf{1}\mathbf{1}^\top \right) \tilde{\nabla} F^t.$$

Therefore, we can obtain the following consensus error recursion

$$\Theta_o^{t+1} = \mathbf{A}^{t+1} \Theta_o^t - \gamma_{t+1} \left(\mathbf{I} - (1/n) \mathbf{1}\mathbf{1}^\top \right) \tilde{\nabla} F^t.$$

Then, we aim to link Θ_o^{t+1} to Θ_o^{t-B+1} .

$$\begin{aligned} \Theta_o^{t+1} &= \mathbf{A}^{t+1} \Theta_o^t - \gamma_t \left(\mathbf{I} - (1/n) \mathbf{1}\mathbf{1}^\top \right) \tilde{\nabla} F^{t-1} \\ &= \mathbf{A}^{t+1} \mathbf{A}^t \Theta_o^{t-1} - \gamma_t \mathbf{A}^{t+1} \left(\mathbf{I} - (1/n) \mathbf{1}\mathbf{1}^\top \right) \tilde{\nabla} F^{t-1} - \gamma_{t+1} \left(\mathbf{I} - (1/n) \mathbf{1}\mathbf{1}^\top \right) \tilde{\nabla} F^t \\ &\quad \vdots \\ &= \mathbf{A}^{t+1} \mathbf{A}^t \mathbf{A}^{t-1} \dots \mathbf{A}^{t-B+1} \Theta_o^{t-B+1} - \sum_{s=t-B+1}^t \gamma_{s+1} \mathbf{A}^{s+2} \left(\mathbf{I} - (1/n) \mathbf{1}\mathbf{1}^\top \right) \tilde{\nabla} F^s. \end{aligned}$$

Taking Frobenius norm on both sides and applying the Young's inequality give

$$\begin{aligned} \|\Theta_o^{t+1}\|_F^2 &\leq (1 + \alpha) \|\mathbf{A}^{t+1} \mathbf{A}^t \mathbf{A}^{t-1} \dots \mathbf{A}^{t-B+1}\|^2 \|\Theta_o^{t-B+1}\|_F^2 \\ &\quad + (1 + \alpha^{-1}) \sum_{s=t-B+1}^t \gamma_{s+1}^2 \|\mathbf{A}^{s+2}\|^2 \left\| \left(\mathbf{I} - (1/n) \mathbf{1}\mathbf{1}^\top \right) \tilde{\nabla} F^s \right\|_F^2, \end{aligned}$$

which holds for any $\alpha > 0$. Using A7 and setting $\alpha = \frac{\rho}{1-\rho}$, we have

$$\|\Theta_o^{t+1}\|_F^2 \leq (1 - \bar{\rho}) \|\Theta_o^{t-B+1}\|_F^2 + \sum_{s=t-B+1}^t \gamma_{s+1}^2 \left\| \left(\mathbf{I} - (1/n) \mathbf{1}\mathbf{1}^\top \right) \tilde{\nabla} F^s \right\|_F^2.$$

Similarly, we get

$$\begin{aligned} \|\Theta_o^{t+2}\|_F^2 &\leq (1 - \bar{\rho}) \|\Theta_o^{t-B+2}\|_F^2 + \sum_{s=t-B+2}^{t+1} \gamma_{s+1}^2 \left\| \left(\mathbf{I} - (1/n) \mathbf{1}\mathbf{1}^\top \right) \tilde{\nabla} F^s \right\|_F^2 \\ &\quad \vdots \\ \|\Theta_o^{t+B}\|_F^2 &\leq (1 - \bar{\rho}) \|\Theta_o^t\|_F^2 + \sum_{s=t}^{t+B-1} \gamma_{s+1}^2 \left\| \left(\mathbf{I} - (1/n) \mathbf{1}\mathbf{1}^\top \right) \tilde{\nabla} F^s \right\|_F^2. \end{aligned}$$

Adding these B consensus errors together leads to

$$\begin{aligned} \Theta(t+1, t+B) &\leq (1 - \bar{\rho}) \Theta(t-B+1, t) \\ &\quad + \frac{\gamma_{t-B+1}^2}{\rho} \left\{ \sum_{s=t-B+1}^t \left\| \left(\mathbf{I} - (1/n) \mathbf{1}\mathbf{1}^\top \right) \tilde{\nabla} F^s \right\|_F^2 + \dots + \sum_{s=t}^{t+B} \left\| \left(\mathbf{I} - (1/n) \mathbf{1}\mathbf{1}^\top \right) \tilde{\nabla} F^s \right\|_F^2 \right\}. \end{aligned} \tag{61}$$

Using the inequality (49) in the proof of Lemma 4, we get

$$\mathbb{E}_s \left\| \left(\mathbf{I} - (1/n) \mathbf{1}\mathbf{1}^\top \right) \tilde{\nabla} F^s \right\|_F^2 \leq d_1 + d_2 \|\tilde{\boldsymbol{\theta}}^s\|^2 + c_3 \|\Theta_o^s\|_F^2,$$

where $d_1 := 9n(\sigma^2 + \varsigma^2)$, $d_2 := 12n(\sigma^2 + \varsigma^2)$ and $c_3 = 12\sigma^2 + 18L^2(1 + \epsilon_{\max})^2$. Then, we have

$$\begin{aligned} \sum_{s=t-B+1}^t \mathbb{E} \left\| \left(\mathbf{I} - (1/n)\mathbf{1}\mathbf{1}^\top \right) \tilde{\nabla} F^s \right\|_F^2 &\leq \sum_{s=t-B+1}^t \mathbb{E} \left[d_1 + d_2 \|\tilde{\boldsymbol{\theta}}^s\|^2 + c_3 \|\boldsymbol{\Theta}_o^s\|_F^2 \right] \\ &= Bd_1 + d_2 \sum_{s=t-B+1}^t \mathbb{E} \|\tilde{\boldsymbol{\theta}}^s\|^2 + c_3 \sum_{s=t-B+1}^t \mathbb{E} \|\boldsymbol{\Theta}_o^s\|_F^2. \end{aligned}$$

Substituting back to (61) give us

$$\begin{aligned} \boldsymbol{\Theta}(t+1, t+B) &\leq (1 - \bar{\rho})\boldsymbol{\Theta}(t-B+1, t) + \frac{\gamma_{t-B+1}^2}{\rho} \left\{ B^2 d_1 + d_2 [\tilde{\boldsymbol{\theta}}(t-B+1, t) + \cdots + \tilde{\boldsymbol{\theta}}(t, t+B)] \right. \\ &\quad \left. + c_3 [\boldsymbol{\Theta}(t-B+1, t) + \cdots + \boldsymbol{\Theta}(t, t+B)] \right\}. \end{aligned}$$

The above can be simplified to

$$\begin{aligned} \boldsymbol{\Theta}(t+1, t+B) &\leq (1 - \bar{\rho})\boldsymbol{\Theta}(t-B+1, t) + \frac{\gamma_{t-B+1}^2}{\rho} \left\{ B^2 d_1 + d_2 B [\tilde{\boldsymbol{\theta}}(t+1, t+B) + \tilde{\boldsymbol{\theta}}(t, t+B)] \right. \\ &\quad \left. + c_3 B [\boldsymbol{\Theta}(t-B+1, t) + \boldsymbol{\Theta}(t+1, t+B)] \right\}. \end{aligned}$$

Setting $\sup_{k \geq 1} \gamma_k \leq \frac{\bar{\rho}}{\sqrt{2c_3 B}}$ and rearranging terms give us

$$\begin{aligned} \boldsymbol{\Theta}(t+1, t+B) &\leq \frac{1 - \bar{\rho}/2}{1 - Bc_3 \gamma_{t-B+1}^2 / \bar{\rho}} \boldsymbol{\Theta}(t-B+1, t) \\ &\quad + \frac{\gamma_{t-B+1}^2}{\rho - Bc_3 \gamma_{t-B+1}^2} \left\{ B^2 d_1 + d_2 B [\tilde{\boldsymbol{\theta}}(t-B+1, t) + \tilde{\boldsymbol{\theta}}(t+1, t+B)] \right\}, \end{aligned}$$

which gives us desired upper bound for $\boldsymbol{\Theta}(t+1, t+B)$. \square

Convergence of $\tilde{\boldsymbol{\theta}}^t$ to $\boldsymbol{\theta}^{PS}$ with Time varying graph. We conclude our proof sketch through analyzing the following Lyapunov function. For any $t \geq 0$, we define:

$$\mathcal{L}_{t+1}^{t+B} := \tilde{\boldsymbol{\theta}}(t+1, t+B) + \boldsymbol{\Theta}(t+1, t+B) \geq 0.$$

Combing Lemma 8 and 9 leads to

$$\begin{aligned} &\left(1 - Bc_1 \frac{\gamma_{t+1}}{n} - Bc_2 \frac{\gamma_{t+1}^2}{n} \right) \boldsymbol{\Theta}(t+1, t+B) + \left(1 - \frac{d_2 B \gamma_{t-B+1}^2}{\rho - Bc_3 \gamma_{t-B+1}^2} \right) \tilde{\boldsymbol{\theta}}(t+1, t+B) \\ &\leq \left(\frac{1 - \bar{\rho}/2}{1 - Bc_3 \gamma_{t-B+1}^2 / \bar{\rho}} + Bc_1 \frac{\gamma_{t+1}}{n} + Bc_2 \frac{\gamma_{t+1}^2}{n} \right) \boldsymbol{\Theta}(t-B+1, t) \\ &\quad + \left((1 - \tilde{\mu} \gamma_{t+B})^B + \frac{d_2 B \gamma_{t-B+1}^2}{\rho - Bc_3 \gamma_{t-B+1}^2} \right) \tilde{\boldsymbol{\theta}}(t-B+1, t) + \frac{B^2 d_1 \gamma_{t-B+1}^2}{\rho - Bc_3 \gamma_{t-B+1}^2} + \frac{2B\sigma^2}{n} \gamma_{t+1}^2. \end{aligned} \tag{62}$$

We focus on the l.h.s. of above inequality. If the step size satisfies

$$\sup_{k \geq 1} \gamma_k \leq \min \left\{ \frac{c_1}{c_2}, \sqrt{\frac{\bar{\rho}}{2Bc_3}}, \frac{\bar{\rho}c_1}{n} \right\}$$

then, the l.h.s. of (62) can be lower bounded by

$$\text{l.h.s. of (62)} \geq \left(1 - 2Bc_1 \frac{\gamma_{t+1}}{n} \right) \left[\boldsymbol{\Theta}(t+1, t+B) + \tilde{\boldsymbol{\theta}}(t+1, t+B) \right].$$

Next, we consider the r.h.s. of (62). Suppose that $\sup_{k \geq 1} \gamma_k \leq \sqrt{\frac{\bar{\rho}}{(4-\bar{\rho})Bc_3}}$, it holds

$$\frac{1 - \bar{\rho}/2}{1 - Bc_3\gamma_{t-B+1}^2/\bar{\rho}} \leq 1 - \bar{\rho}/4, \quad \frac{B^2d_1\gamma_{t-B+1}^2}{\rho - Bc_3\gamma_{t-B+1}^2} \leq \frac{2B^2d_1}{\rho}\gamma_{t-B+1}^2.$$

If step size also satisfies

$$\sup_{k \geq 1} \gamma_k \leq \min \left\{ \frac{1}{\sqrt{b}}, \frac{\tilde{\mu}\bar{\rho}}{2^{2B+1}d_2B} \right\},$$

where b such that $\gamma_k^2/\gamma_{k+1}^2 \leq 1 + b\gamma_{k+1}^2$, then it holds:

$$\begin{aligned} & \text{r.h.s. of (62)} \\ & \leq \left(1 - \frac{\bar{\rho}}{4} + 2Bc_1\frac{\gamma_{t+1}}{n}\right) \Theta(t-B+1, t) + \left(1 - \frac{\tilde{\mu}\gamma_{t+B}}{2}\right) \tilde{\Theta}(t-B+1, t) \\ & \quad + \frac{2B^2d_1}{\rho}\gamma_{t-B+1}^2 + \frac{2B\sigma^2}{n}\gamma_{t+1}^2. \end{aligned}$$

Combining the above inequalities lead to:

$$\begin{aligned} & \left(1 - 2Bc_1\frac{\gamma_{t+1}}{n}\right) \left[\Theta(t+1, t+B) + \tilde{\Theta}(t+1, t+B)\right] \leq \left(1 - \frac{\bar{\rho}}{4} + 2Bc_1\frac{\gamma_{t+1}}{n}\right) \Theta(t-B+1, t) \\ & \quad + \left(1 - \frac{\tilde{\mu}\gamma_{t+B}}{2}\right) \tilde{\Theta}(t-B+1, t) + \frac{2B^2d_1}{\rho}\gamma_{t-B+1}^2 + \frac{2B\sigma^2}{n}\gamma_{t+1}^2. \end{aligned}$$

If the step size satisfying

$$\sup_{k \geq 1} \gamma_k \leq \frac{\bar{\rho}}{8Bc_1/n + 2\tilde{\mu}},$$

then the main recursion can be simplified as

$$\begin{aligned} & \left(1 - 2Bc_1\frac{\gamma_{t+1}}{n}\right) \left[\Theta(t+1, t+B) + \tilde{\Theta}(t+1, t+B)\right] \\ & \leq \left(1 - \frac{\tilde{\mu}\gamma_{t+B}}{2}\right) \left[\Theta(t-B+1, t) + \tilde{\Theta}(t-B+1, t)\right] + \frac{2B^2d_1}{\rho}\gamma_{t-B+1}^2 + \frac{2B\sigma^2}{n}\gamma_{t+1}^2. \end{aligned}$$

Dividing $(1 - 2Bc_1\frac{\gamma_{t+1}}{n})$ for the both sides, we obtain that

$$\mathcal{L}_{t+1}^{t+B} \leq \frac{(1 - \tilde{\mu}\gamma_{t+B}/2)}{1 - 2Bc_1\gamma_{t+1}/n} \mathcal{L}_{t-B+1}^t + \left(\frac{2B^2d_1}{\rho} + \frac{2B\sigma^2}{n}\right) \frac{\gamma_{t-B+1}^2}{(1 - 2Bc_1\gamma_{t+1}/n)}.$$

Observe that with sufficiently small step size, the above recursion can be simplified to give a similar form as (25). Solving the recursion then lead to $\mathcal{L}_{t+1}^{t+B} = \mathcal{O}(\gamma_{t-B+1})$ and the convergence of $\tilde{\Theta}(t+1, t+B) \rightarrow 0$.

Lastly, we remark that the above analysis only gives a crude bound to the convergence of DSGD-GD in the time varying graph setting. It is possible to give tighter bounds through further optimizing the constants in the above analysis.

H Extension to Local Distributions Influenced by All Agents

This section outlines how to extend our analysis to the scenario when the local distributions $\mathcal{D}_i(\cdot)$ are simultaneously influenced by other agents in the network similar to the competitive Multi-PfD considered by [Narang et al., 2022, Piliouras and Yu, 2022].

We define the concatenated decision vector $\boldsymbol{\vartheta} := (\boldsymbol{\theta}_1, \dots, \boldsymbol{\theta}_n) \in \mathbb{R}^{nd}$ and state the modified consensus Multi-PfD problem (1) as follows

$$\min_{\boldsymbol{\theta}_i \in \mathbb{R}^d, i=1, \dots, n} \frac{1}{n} \sum_{i=1}^n \mathbb{E}_{Z_i \sim \mathcal{D}_i(\boldsymbol{\vartheta})} [\ell(\boldsymbol{\theta}_i; Z_i)] \quad \text{s.t.} \quad \boldsymbol{\theta}_i = \boldsymbol{\theta}_j, \quad \forall (i, j) \in E. \quad (63)$$

With a slight abuse of notation, we also define $f_i(\boldsymbol{\theta}; \boldsymbol{\vartheta}) := \mathbb{E}_{Z_i \sim \mathcal{D}_i(\boldsymbol{\vartheta})}[\ell(\boldsymbol{\theta}_i; Z_i)]$.

Following [Narang et al., 2022], we consider the following modification to A3:

A8. For any $i = 1, \dots, n$, there exists a constant $\epsilon_i > 0$ such that

$$\mathcal{W}_1(\mathcal{D}_i(\boldsymbol{\vartheta}), \mathcal{D}_i(\boldsymbol{\vartheta}')) \leq \epsilon_i \|\boldsymbol{\vartheta} - \boldsymbol{\vartheta}'\|, \quad \forall \boldsymbol{\vartheta}', \boldsymbol{\vartheta} \in \mathbb{R}^{nd}, \quad (64)$$

where $\mathcal{W}_1(\mathcal{D}, \mathcal{D}')$ denotes the Wasserstein-1 distance between the distributions $\mathcal{D}, \mathcal{D}'$.

Specifically, we notice that if $\boldsymbol{\vartheta}$ satisfies the consensus constraint, i.e., $\boldsymbol{\vartheta} = \mathbf{1}_n \otimes \boldsymbol{\theta} = (\boldsymbol{\theta}, \dots, \boldsymbol{\theta})$, then A8 is equivalent to A3 with the latter's sensitivity parameter given by $\epsilon'_i = \sqrt{n}\epsilon_i$ since $\|\mathbf{1}_n \otimes \boldsymbol{\theta} - \mathbf{1}_n \otimes \boldsymbol{\theta}'\| = \sqrt{n}\|\boldsymbol{\theta} - \boldsymbol{\theta}'\|$. This observation immediately leads to the following corollary of Proposition 1:

Corollary 1. Under A1, A2, A8. Define the map $\mathcal{M} : \mathbb{R}^d \rightarrow \mathbb{R}^d$

$$\mathcal{M}(\boldsymbol{\theta}) = \arg \min_{\boldsymbol{\theta}' \in \mathbb{R}^d} \frac{1}{n} \sum_{i=1}^n f_i(\boldsymbol{\theta}'; \mathbf{1}_n \otimes \boldsymbol{\theta}) \quad (65)$$

If $\sqrt{n}\epsilon_{\text{avg}} < \mu/L$, then the map $\mathcal{M}(\boldsymbol{\theta})$ is a contraction with the unique fixed point $\boldsymbol{\theta}^{PS} = \mathcal{M}(\boldsymbol{\theta}^{PS})$. If $\sqrt{n}\epsilon_{\text{avg}} \geq \mu/L$, then there exists an instance of (11) where $\lim_{T \rightarrow \infty} \|\mathcal{M}^T(\boldsymbol{\theta})\| = \infty$.

The proof is attained by simply observing that if $\boldsymbol{\theta}_i = \boldsymbol{\theta}_j$ (as constrained by (65) (and (63)), then A8 is equivalent to A3 with $\epsilon'_i = \sqrt{n}\epsilon_i$.

Comparison to [Narang et al., 2022]. Notice that in [Narang et al., 2022], the existence of a performative stable equilibrium requires $\sqrt{\sum_{i=1}^n \epsilon_i^2} < \mu/L$. Meanwhile, Corollary 1 requires $(1/\sqrt{n}) \sum_{i=1}^n \epsilon_i < \mu/L$. Due to norm equivalence, we have

$$(1/\sqrt{n}) \sum_{i=1}^n \epsilon_i \leq \sum_{i=1}^n \epsilon_i^2.$$

Thus, the consensus constrained performative stable solution in cooperative Multi-PfD will be attainable under a more relaxed condition than the competitive Multi-PfD.

DSGD-GD Algorithm for (63). The extension of Theorem 1 to (63) via the DSGD-GD algorithm is more involved and thus the details are skipped in this brief discussion. However, it remains straightforward to extend the analysis through a careful modification of Lemma 3 with A8. In particular, one only needs to pay attention to the use of A8 in (37) and (40) for the proof.

Remarks. Lastly, we emphasize that as explained in the main paper, the original scenario considered by (1) and A3 is relevant to the decentralized learning scenario of the current paper. It captures the effects of ‘geographical’ barriers where the population of users are not simultaneously influenced by all agents. Nevertheless, a future direction is to study the Multi-PfD problem (cooperative or competitive) where users can be influenced by the decisions from a *few* neighboring agents.